2021-04

Stapp Car Crash Journal, Vol. 65 (November 2021), pp. 49-90

Analysis of Lap Belt Fit to Human Subjects using CT Images

Yoshihiko Tanaka, Atsushi Nakashima, Haijie Feng and Koji Mizuno
Nagoya University

Minoru Yamada, Yoshitake Yamada, Yoichi Yokoyama and Masahito Jinzaki
Keio University School of Medicine

ABSTRACT – In vehicle collisions, the lap belt should engage the anterior superior iliac spine (ASIS). In this study, three-dimensional (3D) shapes of bones and soft tissues around the pelvis were acquired using a computed tomography (CT) scan of 10 male and 10 female participants wearing a lap belt. Standing, upright sitting, and reclined postures were scanned using an upright CT and a supine CT scan system. In the upright sitting posture, the thigh height was larger with a higher BMI while the ASIS height did not change significantly with BMI. As a result, the height of the ASIS relative to the thigh (ASIS-thigh height) became smaller as the BMI increased. Because the thigh height of females was smaller than that of males, the ASIS-thigh height was larger for females than for males. As the ASIS-thigh height was larger, the overlap of the lap belt with the ASIS increased. Thus, the lap belt overlapped more with the ASIS for the females than for the males. The abdomen outer shape is characterized by the trouser cord formed valley, the torso/thigh junction, and the anterior convexity formed between them depending on the adipose tissues. The abdomen outer shapes changed from the standing, the reclined posture to the upright sitting posture. In the reclined sitting posture, the lap belt is positioned upward and rearward relative to the ASIS, and the overlap of the lap belt with the ASIS was smaller compared to the upright posture.

KEYWORDS – Safety belts, Lap belt fit, ASIS, Posture, Computed tomography

INTRODUCTION

A seat belt is a key element of the restraint system for occupant protection in cars, and has been demonstrated to be effective for reducing the risk of fatalities and serious injuries in vehicle crashes (Kahane 2000). The seat belt controls an occupant's kinematics and prevents contact of the occupant within the car interior. During vehicle frontal impacts, the lap belt should engage the anterior edge of the ilium, and the anterior superior iliac spine (ASIS) can be a hook of the lap belt during impacts. Submarining is defined as the lap belt slipping off from the ASIS. The lap belt slipping off the ASIS and thereby penetrating the abdominal region can cause serious injuries to the abdomen (Lamielle et al., 2006). During impacts, as the pelvis moves forward and downward into the seat while rotating backward causing the angle of the lap belt to become shallower, the contact force component of the lap belt against the pelvis in the tangential direction changes from an inferior to a superior direction. Leung (1981) and Horsch (1989) proposed that the lap belt starts to slip when the tangential force of the lap belt on the anterior edge of the iliac bone exceeds the maximum friction force in the superior direction. This theory is based on the contact between the belt and the rigid body. Probably, the shear deformation of the soft tissue over the ASIS can also affect the lap belt slippage. The angle of the lap belt relative to the pelvis is a critical parameter for predicting submarining. Countermeasures for preventing submarining (e.g., occupant position, posture, lap belt anchorage position, seat belt pretentioner, and seat pan design) have been investigated in many studies (Leung et al., 1982; Rouhana et al., 1989; Östling et al., 2017).

Though submarining has been investigated in many studies by using crash test dummies, some studies investigated the lap belt path around the pelvis of human subject participants. Reed et al. (2012) measured the lap belt location and surface landmarks of participants sitting on the front seat of a car by using a coordinate digitizer. The BMI had the greatest effects on the belt fit measures while the participant's

Koji Mizuno, Nagoya University, School of Engineering
Furo-cho, Chikusa-ku, Nagoya 464-8603, Japan
Electronic mail: kmizuno@mech.nagoya-u.ac.jp

sex did not significantly affect the belt fit. The lap belt of obese participants was located further away from the ASIS in the anterosuperior directions. In a series of frontal impact tests using post mortem human subjects (PMHSs), the lap belt penetrated the abdominal area of the obese occupants due to poor lap belt location relative to the pelvis (Kent 2010). Park et al. (2018) reported that the lap belt was positioned lower relative to the ASIS in the Hybrid III Adult Male 50th (AM50) and Hybrid III Adult Female 05th (AF05) dummies than in participants. They suggested that vehicle crash tests using the Hybrid III dummies overestimate the engagement of the lap belt with the pelvis of humans.

As for a lap belt's fit to the pelvis, the lap belt overlaps with the ASIS of a Hybrid III AM50 dummy that is commonly used in vehicle crash tests. Hence, many studies of submarining using Hybrid III dummies have assumed that the lap belt engages with the ASIS in the initial stage, and then it slips off the ASIS during impacts. However, submarining also occurs when the lap belt is above the ASIS before impacts and does not engage the ASIS. Wells et al. (1986) surveyed the lap belt fit of volunteers, reporting that the degree of lap belt-ASIS overlap was frequently insufficient. Forty-two percent (42%) of the lap belt centerline was above the ASIS, and 89% partly overlapped the ASIS. Even though the lap belt does not overlap the ASIS initially, the lap belt can be designed to engage the ASIS by incorporating a lap belt pretensioner in the front seats of some cars. Mizuno et al. (2018, 2019) surveyed the locations of the lap belt relative to the ASIS for 10 male participants sitting in the rear seat of a small car. The lower edge of the lap belt was higher than the ASIS for four participants. Though the lap belt engagement with the ASIS is essential in the rear seat because the knees are not restrained by the knee bolster, Mizuno's study implied that the lap belt may not engage the ASIS in the initial stage of an impact for some occupants sitting in the rear seat. They also suggested from analyzing finite element (FE) impact simulations that the overlap of the lap belt with the ASIS was poor and submarining occurred for occupants with a flat abdomen and large thigh diameter.

In future autonomous vehicles, occupants likely may sit in various postures, e.g., highly reclined postures. Hence, the demands of understanding the safety of occupants in the various postures are increasing. Reed et al. (2019) measured the belt fit for participants in a front seat based on digitized surface landmarks. They showed that the pelvis angle inclined rearward and the lumbar spine flexion decreased with reclined postures. FE analyses were conducted for occupants in reclined sitting postures in frontal impacts, and the results showed that the pelvis rotated rearward with large forward displacement, and the lap belt slid over the ASIS (Lin et al. 2018, Rawska et al. 2019, 2020). The postures of the pelvis and lumbar spine as well as the lap belt fit in the reclined sitting postures are significant parameters in these simulations, but the available information for these parameters on various occupants are still not sufficient yet.

Izumiyama et al. (2018, 2019, 2020) measured the ASIS location of 75 participants. A car front seat was set in an X-ray facility, and participants sat on this seat in a driving posture. The skeletal alignment was measured, and they found that the pelvis angle was related to the curvature of the lumbar spine: the pelvis of a low-BMI participant was inclined to tilt rearward with C-shape lumbar spine. Their finite element analyses also showed that the lap belt tends to slip off the ASIS of the pelvis of an occupant with a rear-tilted pelvis posture.

Because occupant protection in various seating postures is important toward autonomous vehicles, understanding the three-dimensional (3D) geometrical relation of the lap belt with the pelvis is needed in order to design the lap belt to restrain the pelvis effectively. However, it is difficult to accurately determine the position of landmarks of bones by estimating from the outer surface using coordinate digitizers or structured light 3D scanners. Using palpations, pelvis shapes, and posture as well as the ASIS location under the soft tissue includes errors that cannot be identified easily. In using X-rays, though the bone shapes can be identified in two dimensions, the 3D shape of the pelvis and the soft tissue around the pelvis cannot be obtained, which significantly affects the lap belt location. In this study, 3D shapes of bones and soft tissues around the pelvis for recruited participants were imaged. These were done with the subject in the upright sitting posture and wearing a lap belt and in the standing posture by using an upright computed tomography (CT) scan system which was newly developed. The reclined postures were imaged by a supine CT system. The landmarks of bones around the pelvis in the standing, upright sitting and reclined sitting postures with the lap belt fit were examined from CT images.

METHODS

Participants

The anthropometry of participants around the pelvis and the lap belt fitting geometry were measured from CT data. Participants were recruited through a temporary employment agency. Table 1 presents participant information. The average body mass index (BMI) in Japan is 23.8 kg/m^2 for males and 22.5 kg/m^2 for females according to Japanese Ministry of Health, Labour and Welfare (2019). We recruited 10 male and 10 female participants with a BMI distribution of 5 levels (less than 20, 20-22.5, 22.5-25, 25-30, and 30 kg/m^2 or more). These BMIs were categorized with an emphasis on low BMIs, because in a previous study it was determined that low BMI occupants may fit the lap belt on the abdomen in a slouching sitting posture (Mizuno et al. 2018). Each BMI category includes two participants. The participants wore the same types of upper and lower clothing that patients use in CT scans. They selected the size of the clothing by themselves. The research and procedure of measurements of participants using CT scans were approved by the ethics committee of Keio University School of Medicine (2019-0217) and Nagoya University School of Engineering (19-14). Written informed consent was obtained from the participants using a form approved by the committees.

CT system

Each participant was scanned by CT in three postures: standing posture, upright sitting posture, and reclined sitting posture. The upright CT scan system that was developed by Keio University and Canon Medical Systems Corporation (Jinzaki et al. 2020) was applied to scanning in a standing posture and an upright sitting posture of participants (Fig. 1). In this upright CT scan system, a transverse 320 row-detector gantry moves vertically, and can scan a human subject in the acrylic cylinder of 700 mm of inner diameter. The field of view of the scan is 500 mm in diameter. A wooden seat can be installed inside the acrylic cylinder, and a human subject can be scanned in a seated posture. In addition, a supine CT scan system was used to take images in the reclined sitting posture. The gantry was tilted and scanned 6 times to take the images around the pelvis because the range of oblique motion of the gantry was limited (Fig. 4). These 6 images were combined into one image. As the field of view was limited in the diameter, the abdomen in the anterior area for high BMI participants was missing. The average radiation dose per person in a total of standing, sitting, and reclined postures was 15.0 mSv (standing 5.0 mSv, sitting 4.6 mSv, and reclined 5.4 mSv).

Table 1 Participant data

	Height (cm)	Weight (kg)	BMI (kg/m^2)	Age
Male 01	174	57	18.8	48
Male 02	171.5	98.5	33.5	21
Male 03	169.2	50.5	17.6	27
Male 04	165	93	34.2	33
Male 05	179	75	23.4	30
Male 06	168	78	27.6	41
Male 07	168.8	63	22.1	43
Male 08	171	85	29.1	36
Male 09	168	70	24.8	47
Male 10	168.3	63.1	22.3	22
Average (male)	170.3	73.3	25.4	34.8
SD	3.7	14.8	5.4	9.3
Female 01	155	55	22.9	33
Female 02	167	63	22.6	37
Female 03	160	45	17.6	27
Female 04	160	54	21.1	25
Female 05	166	52	18.9	46
Female 06	157	53	21.5	37
Female 07	161	82	31.6	48
Female 08	148	59	26.9	30
Female 09	160	80	31.3	33
Female 10	175	80	26.1	46
Average (female)	160.9	62.3	24.1	36.2
SD	6.9	12.8	4.6	7.8

Seat Setting

Fig. 2 shows the geometry of the seat and the anchorage and the buckle of the lap belt. Fig. 3 shows the situations for the CT scans of a participant in the standing, upright sitting posture, and the reclined sitting postures. When imaging the upright sitting posture in the standing CT, a lap belt without shoulder belt was installed on the seat surface. The webbing of a production seat belt with a width of 47 mm was used. The outboard and inboard belt (buckle side) anchor positions were based on the front seat of a small car. To avoid metal artifacts for CT imaging, a resin buckle was used and the belt fixing jigs in both sides of the lap belt were made of Styrofoam. A pulling force was not added for the lap belt.

In the upright sitting posture, the anchor position was decided as follows: using a CAD system, the THOR AM50 dummy was seated on the wooden seat of the upright CT scan system (a horizontal seat with a seat back angle of 90 degrees) so that the dummy's back touches the seat back, and the hip point of the THOR dummy was measured. The anchor position was set to be the same as the anchor position with respect to the

Fig. 1 The upright CT scan system. The gantry position moves from upward (left) to downward (right).

hip point of the THOR dummy seated in the small car (see Fig. 2(c)). The lap belt was fitted to the THOR dummy, and the contact point of the lap belt with the pelvis soft tissue was identified. A line was drawn from the contact point to the lap belt anchorage point. The intersection between this line and the seat surface was determined, and this intersection was reflected as the attachment point of the lap belt at the fixing jig in the wooden seat of the CT.

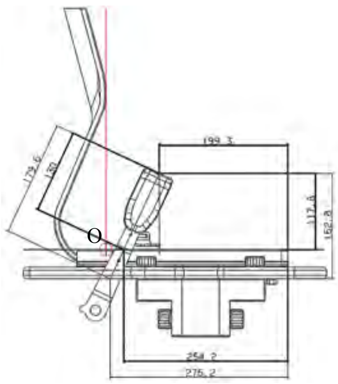

(a) Upright sitting posture

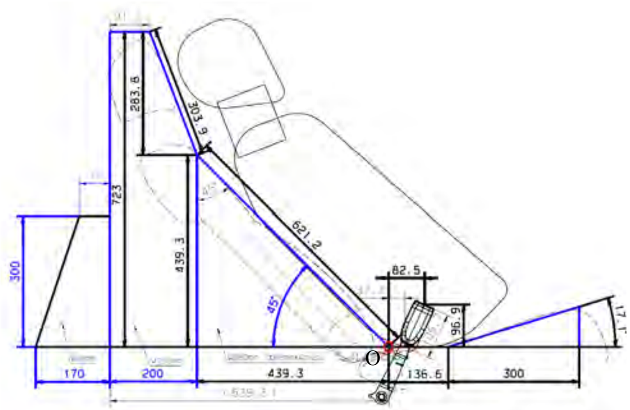

(b) Reclined posture

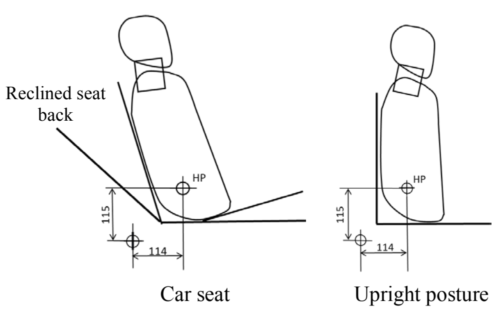

(c) Belt anchor point from the hip point

Fig. 2 Geometry of seat and lap belt for upright sitting and reclined sitting posture. The origin O of the seat coordinate system coincides with the cross line between the seat and the seat back.

In the reclined sitting posture measured by the supine CT scanner system, the reclined seat was made of urethane and was put on the patient bed of CT without any fixation. The angles of the seat back and seat

(a) Standing posture

(b) Upright sitting posture

(c) Reclined posture

Fig. 3 Three participants' postures during measurement using the upright CT scan and supine CT scan system.

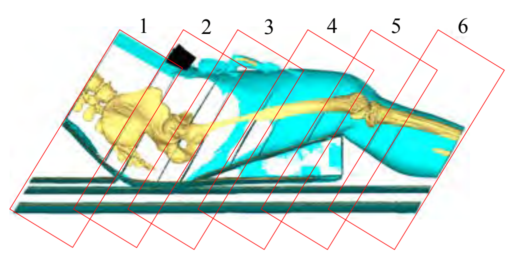

Fig. 4 CT scan of reclined posture. The area surrounded by the red lines was scanned in one shot by combination of the gantry motion and the bed longitudinal motion.

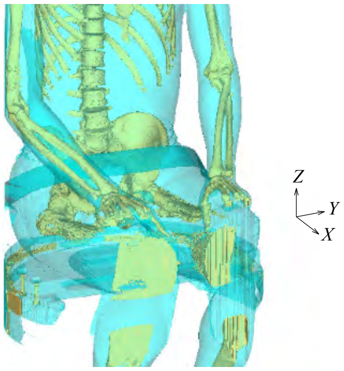

Fig. 5 CT scan image of the upright sitting posture in the upright CT scan system. Note that the anterior area of the knees and tibias are not included due to the limited scan range in the cylinder.

surface were 45 degrees and 17.1 degrees, respectively. The positions of the anchor position with respect to the seat reference point (hip point) were the same as that for the upright sitting posture (see Fig. 2(c)).

Detailed instructions were not provided to participants for the standing and sitting postures. Participants were asked to wear a lap belt using their usual location, and by adjusting the length of the lap belt by themselves. The CT images in the DICOM (**D**igital **I**maging and **CO**mmunications in **M**edicine) format were analyzed using Materialise Mimics. The areas of bones, soft tissues, and lap belt were separated based on the Hounsfield unit (see Fig. 5).

Measurements

The anthropometry and the lap belt positions were measured in the data of CT (Fig. 6). The sizes of the pelvis, which were represented by the pelvis height (from the top of the ilium to the bottom of the ischium) as well as by the width of the right and left ASIS, were compared among participants. The thigh height (i.e., the anterior-posterior diameter of the thigh in the sitting posture) was also measured at the torso-thigh junction in the sagittal plane which went through the ASIS. The ASIS flesh margin was measured from the ASIS to the outer surface of the abdomen in the ASIS-PSIS direction projected on to the sagittal plane through the ASIS. However, for three participants (Male 04, 08, 10) in a sitting position, the ASIS was lower than the torso/thigh junction, and the extension of the ASIS-PSIS line intersected the top of the thigh but not the abdominal surface. For these participants, the flesh margin of the ASIS was measured as the distance from the ASIS to the intersection of the ASIS-PSIS line with a line parallel to the *z*-axis through the torso/thigh junction. The standing height and BMI

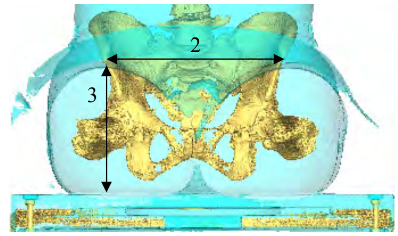

(a) Front view

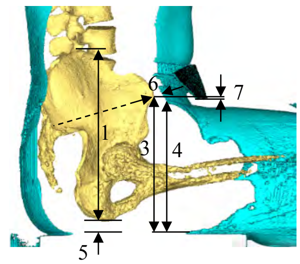

(b) Side view

Fig. 6 CT measurements of anthropometry: 1. Pelvis height, 2. ASIS width, 3. ASIS height, 4. Thigh height, 5. Ischium flesh margin (height of ischium bottom), 6. ASIS flesh margin in anterior direction (*x*), and 7. Overlap of lap belt with the ASIS in the upper direction (*z*).

were used as fundamental variables to express the anthropometry. If there were measurements taken on both sides (e.g., left and right ASIS heights), the average of both sides was calculated.

The pelvis angles in the standing, upright sitting, and reclined sitting postures were compared: the pelvis angle was defined by the angle between the vertical axis and the plane created by anterior edge of the pubis and the right and the left ASIS (Lewinneck plane). The angle of the lumbar spine lordosis angle was measured as the angle between the top of the vertebra body of the third lumbar spine (L3) and the bottom of the vertebra body of L5. This is because L1 and L2 were not included in images of some participants in the reclined sitting posture. The relationship between the pelvis angle and the lumbar spine curvature was examined. The overlap ratio of the lap belt with the ASIS was measured for evaluating the possible engagement of the lap belt with the ASIS in the initial stage of impacts.

Statistical Analysis

Linear regression was applied for the relationship between the objective variables (anthropometry or lap belt fit parameters) and the explanatory variables (e.g., standing height or BMI). The significance of the regression (p-value) and the adjusted R-square R_{adj}^2 were shown. When both the linear regressions for males and females satisfy $p < 0.05$ and $R_{adj}^2 < 0.2$, an analysis of covariance was applied to determine whether the regression lines of males and females were significantly different. In the analysis of covariance, the difference of slopes of the regression lines was tested first ($p < 0.05$); then, if the slopes of the regression lines can be assumed parallel, the equivalence of the intercepts was tested ($p < 0.05$).

The Mann-Whitney U test was also used to compare differences in variables between males and females, and p-value < 0.05 was considered as significant. Spearman's rank correlation matrix was calculated to examine the rank correlation of the order of participants based on the lumbar spine angle in the standing, upright sitting, and reclined sitting group.

To express the lap belt fit by various variables such as the BMI and the standing height, a multiple regression was used. The belt fitting variables such as ASIS-thigh height, the overlap of the lap belt with the ASIS, as well as Lap Belt X (X coordinates of the lap belt upper edge at the midsagittal plane relative to the ASIS). Lap Belt X was used by Reed et al. (2013) to express the lap belt fit on the abdomen. The explanatory variables were selected from the sex, standing height, BMI, and pelvis angle. The stepwise procedure was used for selections of explanatory variables; and the threshold of $p = 0.2$ was used to include and exclude variables.

RESULTS

Images of Outer Surface and Pelvis

Typical bones and skin surfaces obtained in the CT scans of four males and four females are shown in Fig. 7 and Fig. 8, respectively. The upper image is the cross-section of the coronal plane cut at the torso/thigh junction in the upright sitting posture; and the middle image is the sagittal plane which goes through the ASIS. The lower image is the in the reclined sitting posture in the sagittal plane at the ASIS; however, the superior and anterior area of the abdomen could not be obtained because of the limitations of the CT scan area. In the reclined posture, the posterior edge of the ilium and coccyx tilted to make contact along the seat back. Some characteristic differences in pelvis shape between males and females as described in anatomy textbooks (e.g., Khale et al. 1986) can also be observed in Fig. 7 and Fig. 8 as follows:

- The female wings open widely.
- The male pelvis has a more erect iliac bone.
- The angle between the right and the left pubic rami (lower pubic angle) is small in males and is large in females.

Depending on BMI, the differences in the abdomen and the thigh shapes and sizes can be observed; however, the pelvis sizes are comparable irrespective of BMI. There are two valleys observed in the abdominal outer surface in the upright sitting posture (see Fig. 7, Fig. 8 and Appendix A). The upper valley is formed from being compressed by the trouser elastic cord. The lower valley is located at the torso/thigh junction. The abdominal anterior projected convexity is formed between the upper and the lower valleys in the upright sitting posture. While the abdomen of the low-BMI participant is flat, the upper and the lower valleys as well as the convexity in the abdomen are more distinguished in high BMI participants. Even though the same trouser types were used for males and females (size is self-selected), the upper trouser cord valley is located above the ASIS (L4-L5 level) for males, while it is located above the iliac crest and the umbilicus (L3-L4 level) for females in the upright sitting posture. The means and standard deviations of the heights of the trouser cords measured at the midsagittal plane from the seat in the upright sitting posture was 206.0 mm (STD 23.9) for males and 246.4 mm (STD 17.1) for females. They were significantly different for males and females in the Mann-Whitney U test ($p < 0.01$). Hence, the upper valley locates in a more superior location for females than for males, and the abdominal anterior convexity area between the upper and the lower valley is taller in the superior-inferior direction in females than that in males. Besides, some females (e.g., Female 06, and Female 08) have another valley between the upper and the lower valleys in the abdomen.

Males 02, 04, and 08 and Female 10 with a high BMI have a deep valley in the torso/thigh junction which can be referred to as the "abdominal fold" (Lebarbé 2020). Males 04 and 08 have large-diameter thighs, and the torso/thigh junction is located higher than the ASIS. Then, the abdominal folds formed by the trousers' elastic cord position, and the torso/thigh junction coincides with a deeper fold in the high-BMI males. The deepest point inside the abdominal fold is close to the ASIS in the anterior-posterior direction.

In the front view of the upright sitting posture, the cross-sections of the females' thigh shows a large proportion of adipose and a triangular shape that widens laterally toward the seat surface. (see Appendix A).

The participants fitted the lap belt in the path from the side and top (anterior) region of the thigh to the umbilical region of the abdomen. The lap belt was located around the torso/thigh junction at the ASIS area. In the abdominal mid-sagittal area, the lap belt

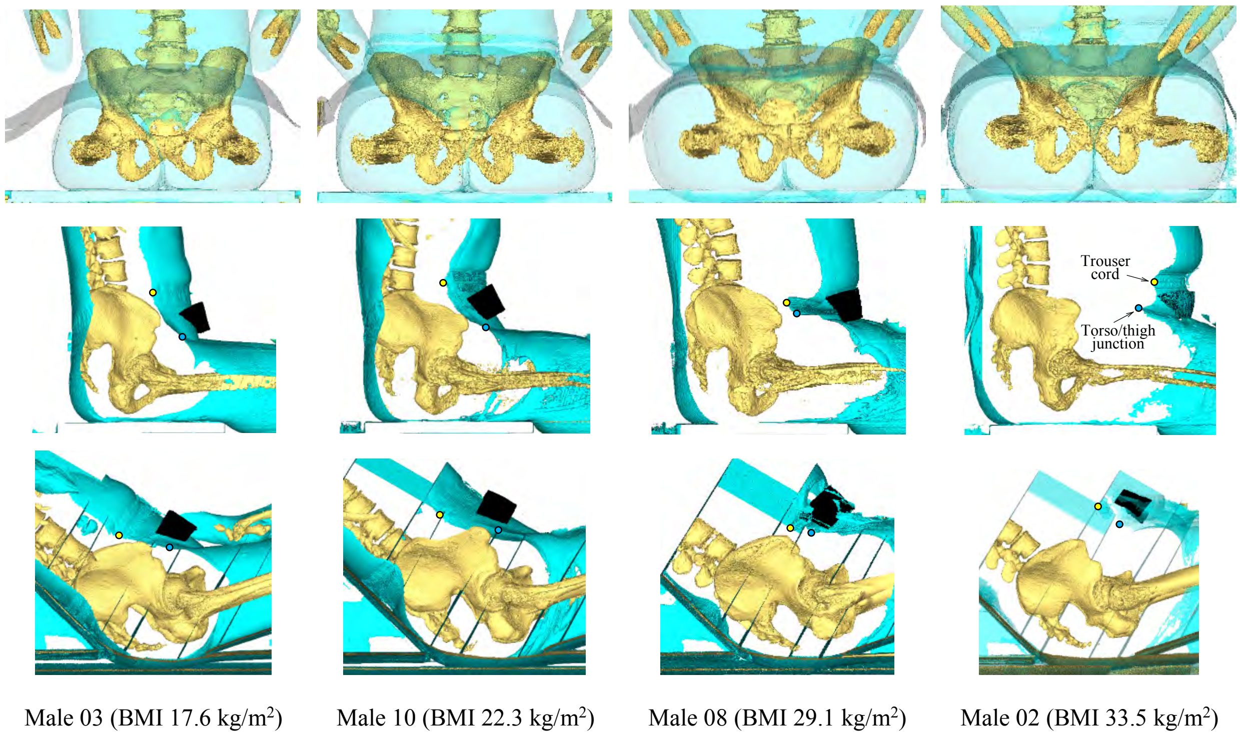

Fig. 7 CT images of bones and surfaces with lap belt for four male participants in upright stitting (coronal and sagittal plane) and reclined sitting postures (sagittal plane that goes through the ASIS). The blue circle is positioned at the torso/thigh junction and the yellow circle is positioned at the trouser cord.

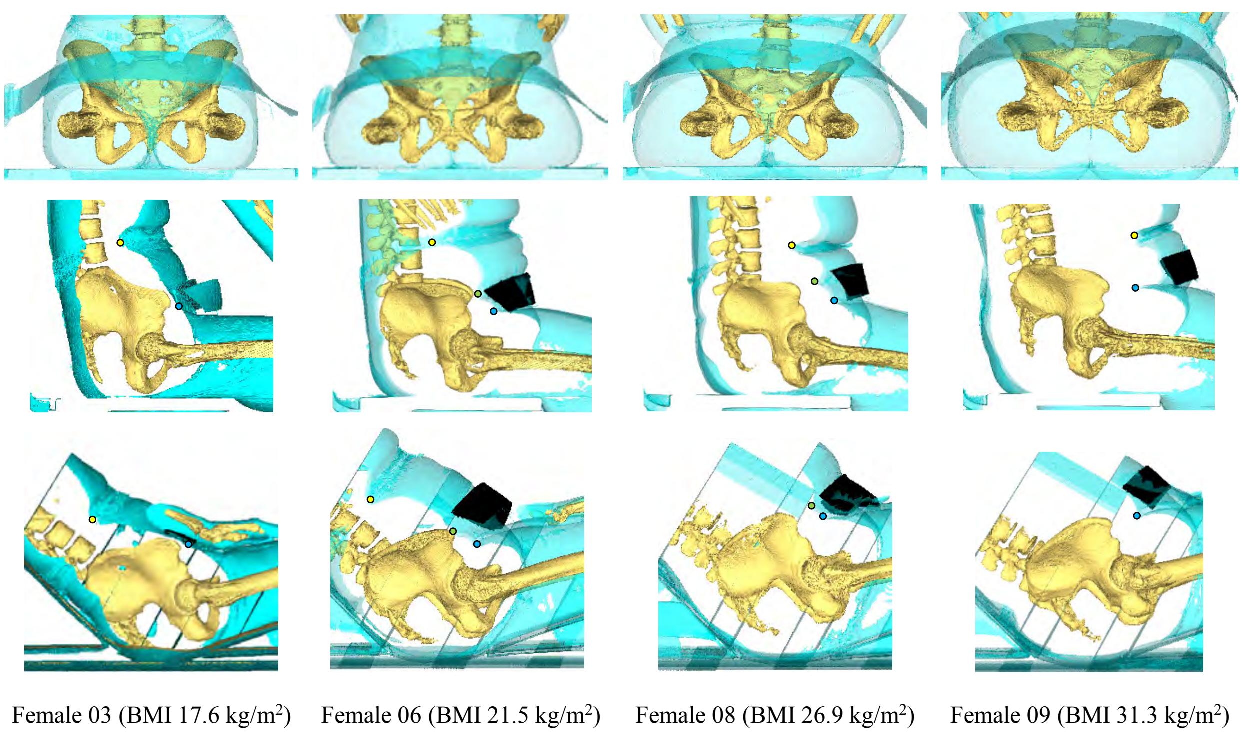

Fig. 8 CT images of bones and surfaces with lap belt for four female participants in upright sitting (coronal and sagittal plane) and reclined sitting postures (sagittal plane that goes through the ASIS). The blue circle is positioned at the torso/thigh junction and the yellow circle is positioned at the trouser cord.

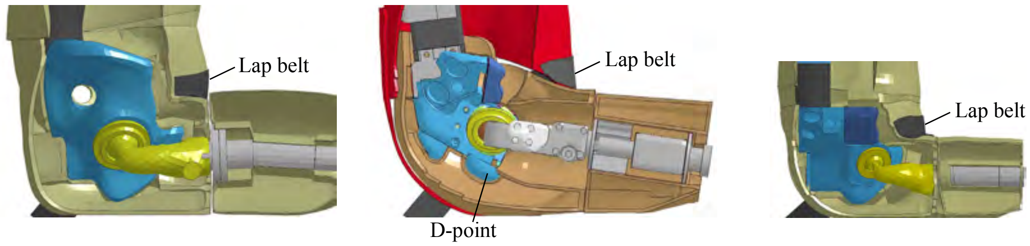

(a) Hybrid III AM50 (b) THOR (c) Hybrid III AF05

Fig. 9 Hybrid III AM50, THOR and Hybrid III AF05 dummies sitting on the plane under gravity. The cross-section of the flesh and the lap belt shown are on the sagittal plane that goes through the ASIS.

was located between the superior and the inferior valley of the umbilical region. The lap belt also was located at the torso-thigh junction in the reclined sitting postures. From the sagittal plane which goes through the ASIS, a gap (belt slack) is observed between the lap belt cross section and the outer surface of the abdomen. In the upright sitting posture, the minimum distance between the lap belt and the outer surface (belt slack) in the x direction is 23.9, 9.7, and 17.0 mm for Male 03 (BMI 17.6), Male 10 (BMI 22.3), and Female 03 (BMI 17.6), respectively; which is larger than 0.8, 1.4, and 1.9 mm, respectively, for Male 08 (BMI 26.9), Male 02 (BMI 33.5), and Female 09 (BMI 31.3). For high-BMI participants (Male 08, Male 02, and Female 09), though the top or bottom edge of the lap belt contacted the outer surface of the abdominal fold, the distance between the lap belt and the deepest point inside the abdominal fold is large.

Flesh Surface and Pelvis of Crash Dummies

FE models of the Hybrid III AM50, THOR AM50 and Hybrid III AF05 dummies seated on the rigid plane are shown in Fig. 9 under the gravity of 9.8 m/s^2. (Note that these FE models have not been validated under accelerations as low as 9.8 m/s^2.) The top surface of the THOR thigh rises toward the torso and covers the ASIS. This thigh shape is closer to the male participants with a middle to high BMI, compared to the Hybrid III AM50 with a 90-degree torso/thigh junction. Though the ischium (pelvis D-points, see Fig. 9) is attached to the bottom of the THOR pelvis, the thickness of pelvis flesh between the D-point and the seat is large in THOR. The Hybrid III AF05 dummy has the flat iliac crest, and the position of the ASIS is high. The same anchor position as used in the upright sitting posture of human subjects in the CT measurements was employed; and the lap belt was fitted around the torso/thigh junction of the dummies. The bottom edge of the lap belt was located below the ASIS, and the belt overlapped the ASIS in the three dummies.

Location of Anatomical Landmarks

The pelvis size (height and ASIS width) is shown in Fig. 10. The pelvis height and the ASIS width are not related to the BMI (pelvis height: $p = 0.625$, $R_{adj}^2 = 0.09$ for males, and $p = 0.855$, $R_{adj}^2 = 0.12$ for females) whereas the pelvis height correlates with the standing height of males and females ($p = 0.035$, $R_{adj}^2 = 0.372$, $p < 0.01$, $R_{adj}^2 = 0.853$). A similar regression line between the pelvis height and the standing height was obtained for males and females. From an analysis of covariance, the regression lines of the pelvis height between males and females are not significantly different ($p = 0.340$). The ASIS width correlates with the standing height for females ($p = 0.012$, $R_{adj}^2 = 0.506$), but not for males ($p = 0.512$, $R_{adj}^2 = -0.063$). The ASIS width of females seems relatively larger than that of males with respect to the same standing height: all data for males were below the regression line for females. The pelvis height of Hybrid III AM50 is comparable to that of males. However, the pelvis height of THOR and Hybrid III AF05 are smaller than that of the human subjects.

Fig. 11 shows the thigh diameter at the base of the thigh in the anterior-posterior direction in the standing posture. The thigh diameter increases with increasing BMI. Based on the regression, for the same BMI, the thigh diameter of females is comparable or slightly larger than that of males. However, from the analysis of covariance, the regression of males and females are not significantly different ($p = 0.220$).

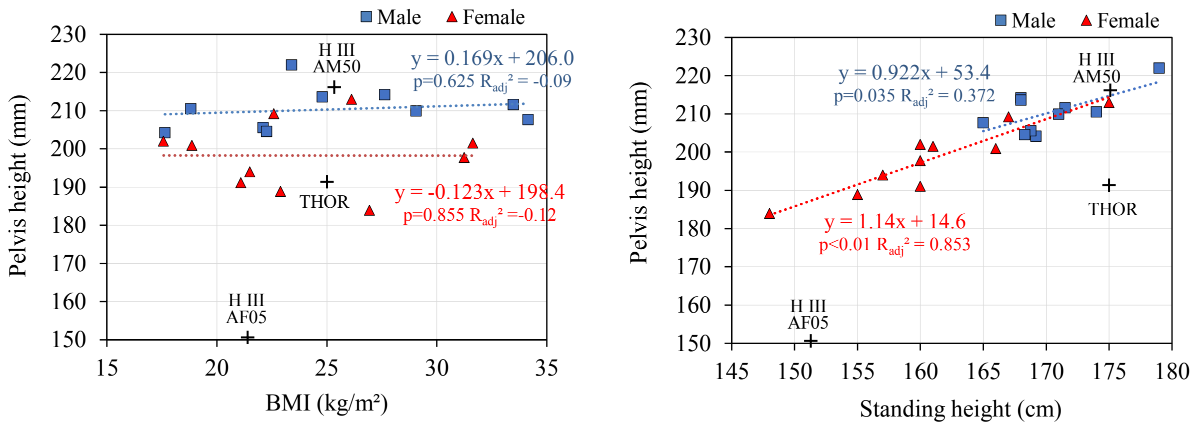

(a) Pelvis height

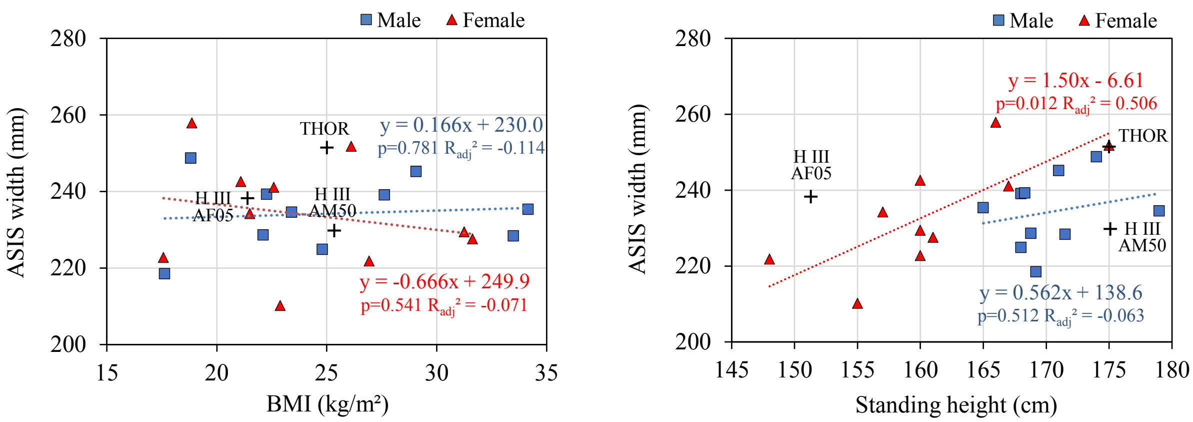

(b) ASIS width

Fig. 10 Pelvis sizes (height and ASIS width) vs. BMI and standing height of participants

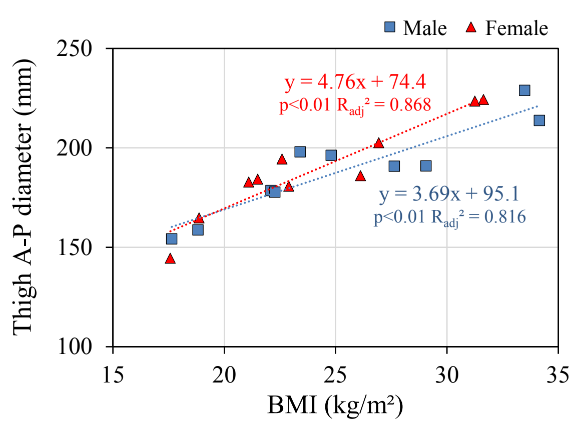

Fig. 11 Thigh diameter in anterior-posterior direction vs. BMI in standing posture

Fig. 12 shows the anthropometry in the upright sitting posture such as the height of the ASIS and the thigh, which are fundamental variables that relate to the overlap of the lap belt with the ASIS. The thigh height from the seat surface tends to increase with higher BMI (see Fig. 12(a)). The thigh height of males is larger than that of females, and the regression line of males and females are significantly different in the analysis of covariance ($p < 0.01$). This tendency is different from that observed in the standing posture; whereby the thigh anterior-posterior diameter is comparable between males and females (see Fig. 11). As shown in Fig. 8 and figures in Appendix A, the cross-section shape of the thigh changes from the standing posture to the upright sitting posture. This implies that the thigh diameter in the anterior-posterior direction decreases a larger degree in females than in males according to the posture change.

The flesh margin below the ischium increases with BMI, and this tendency is comparable between males and females (see Fig. 12(b)). The flesh margin of Hybrid III AM50 (18.1 mm) and AF05 (16.3 mm) is slightly larger than the regression line of the participants, and the flesh margin of the ischium of

THOR is substantially large (50.7 mm). A weak tendency was observed between the height of the ASIS and BMI (see Fig. 12(c)). This is because the flesh margin of the ischium increased with increasing BMI (see Fig. 12(b)), while the pelvis height is independent of BMI (see Fig. 10(a)).

As shown in Fig. 12(d), the ASIS height relative to the thigh height is smaller as the BMI is higher. This is because the higher the BMI, the larger the thigh height. The ASIS-thigh height of females is larger than that of males, and the regression lines of males and females are significantly different in the analysis of covariance ($p < 0.01$). The ASIS is lower than the top of the thigh for six male subjects. In the CT images of the transverse cross section at the level of the ASIS for Males 04, 08, 09, and 10; the anterior area of the thigh can be seen, meaning that the ASIS is lower than the surface at the top of the thigh (see Appendix A).

Multiple regression analysis was used to approximate the ASIS-thigh height (mm) using the standing height, weight, and the pelvis angle. The regression is expressed as:

$$\begin{aligned} \textit{ASIS-thigh height}\ (\text{mm}) &= 16.12\, sex + 1.078\, H \\ &\quad - 1.228\, BMI - 0.7227\, PA - 163.4 \\ &\quad (p < 0.001,\ R_{adj}^2 = 0.743) \end{aligned} \tag{1}$$

where *sex* is male (0) or female (1), *H* is the standing height (cm), *BMI* is the body mass index (kg/m^2), and *PA* is the pelvis angle (degree). All of the above explanatory variables were significant ($p < 0.05$). When the *sex* is female, the standing height *H* increases (pelvis height increase); and when the *BMI* decreases, the *ASIS-thigh height* increases. The standard partial regression coefficients of *sex*, *H, BMI*, and *PA* are 0652, 0.635, −0.501, and −0.515, respectively; thereby these parameters have a comparable effect on the ASIS-thigh height.

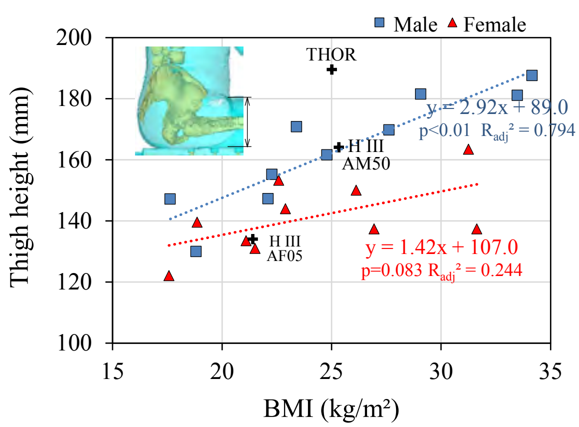

(a) Thigh height

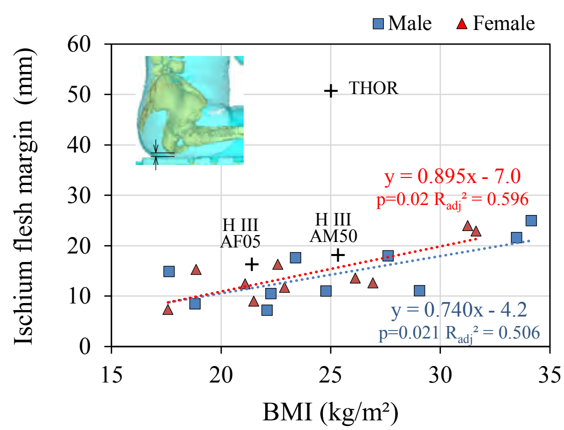

(b) Flesh margin of ischium

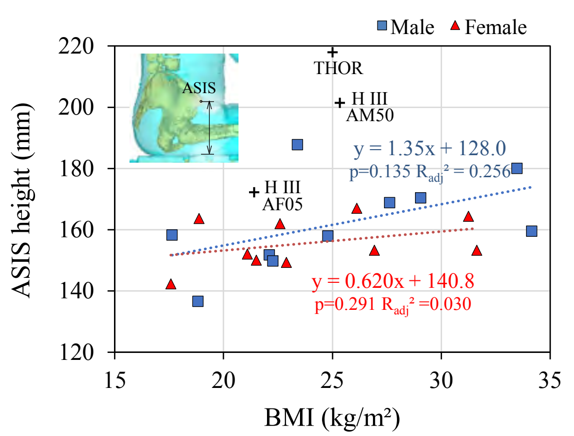

(c) ASIS height

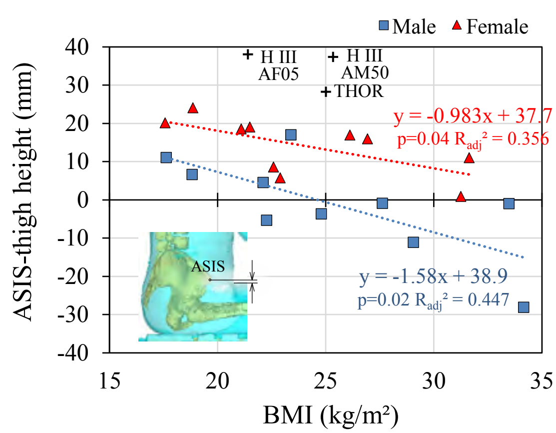

(d) ASIS-thigh height

Fig. 12 Anthropometry related with ASIS height in upright sitting posture

Pelvis and Lumbar Spine Positions and Angles

The position and angle of the pelvis and the lumbar spine were compared in the standing, upright sitting, and reclined postures. Fig. 13 shows the hip position (center of the acetabulum) in the upright sitting and the reclined posture in terms of BMI. The vertical position of the hip point tends to be higher with a higher BMI. The hip point is higher in the reclined sitting than in the upright sitting posture, although there is no clear difference with sex. The X-coordinate of the hip point is not shown because there is no clear trend of the forward position of the hip point by sex or posture, except that for the hip point of females located in the forward position in the upright sitting posture.

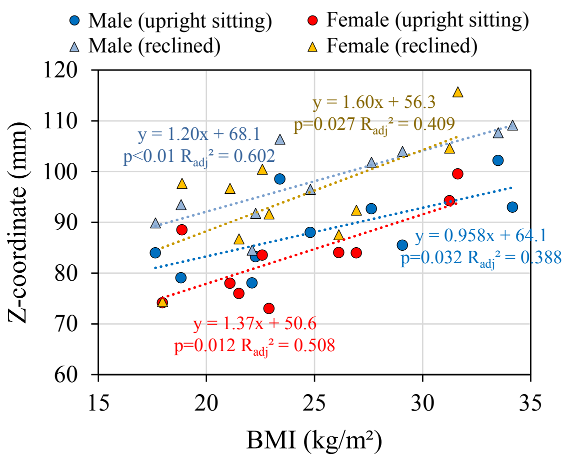

Fig. 13 Vertical position (Z) of the hip point of males and females in the upright sitting and the reclined sitting posture with BMI

As shown in Fig. 14, the pelvis angle varies with the posture of participants. However, a clear trend was not observed for the pelvis angle with BMI. In the male participants, the average pelvis angle was −2.5 degrees (SD 3.6), 13.7 degrees (SD 6.1), and 65.9 degrees (SD 6.5) in the standing, upright sitting, and reclined sitting postures, respectively. In the female participants, the average pelvis angle was 3.5 degrees (SD 4.7), 24.3 degrees (SD 8.5), 65.0 degrees (SD 6.4) in the standing, upright sitting, and reclined sitting postures, respectively. In the upright sitting posture, the pelvis tilt angle of females was larger (the pelvis is tilted rearward) than that of the males. Using the Mann-Whitney U test, the pelvis angles in the upright sitting posture were significantly different between males and females ($p < 0.01$). On the other hand, the pelvis angles were not significantly different for males and females in the standing posture ($p = 0.635$) and reclining posture ($p = 0.684$).

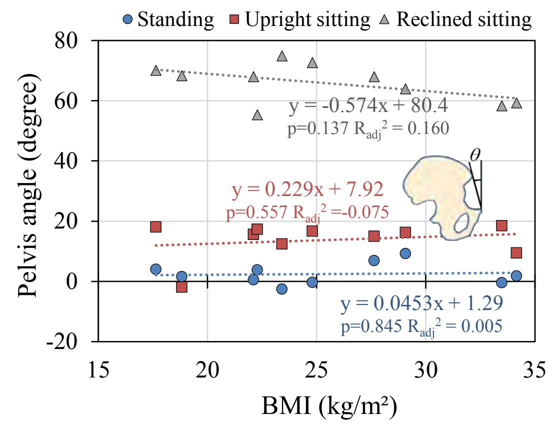

(a) Male

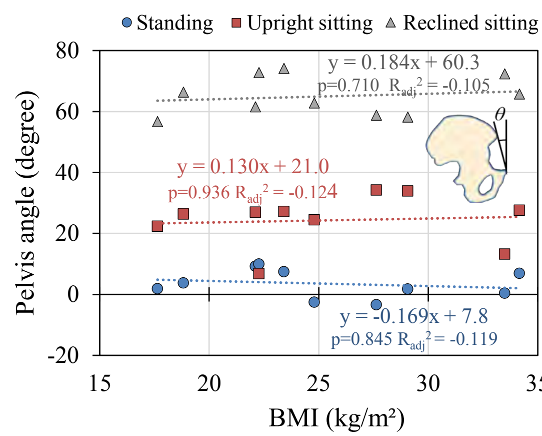

(b) Female

Fig. 14 Pelvis angle of males and females in standing, upright sitting and reclined posture

The rotation center of the pelvis from the upright sitting posture to the reclined sitting posture was calculated from the displacement of the ASIS and pubis in the posture change. Fig. 15 plots the rotation center of the pelvis, the ASIS, and the hip point. Letting the position be expressed by the mean and standard deviation as $(\bar{x} \pm s_x, \bar{z} \pm s_z)$, then the rotation centers of the males and females are (109.2±8.2, 88.4±21.3) and (115.2±10.2, 35.0±64.0), respectively; the hip point of the males and females in the upright sitting posture are (121.0±10.6, 88.4±8.0) and (144.0±22.9, 83.5±8.7), respectively; and the hip point of the males and females in the reclined posture are (118.5±12.4, 98.5±8.5), (120.6±8.4, 94.8±11.2), respectively.

As the sitting posture is changed from the upright sitting to the reclined sitting posture, the average position of the ASIS is higher and more rearward: the average coordinates of the ASIS moved from (158.5, 163.3) to (83.0, 174.1) for males and (162.9, 159.7) to (54.7, 161.5) for females. In addition, the average of the hip point became higher from the upright sitting to the reclined posture: the average height of the hip point moved from 88.4 to 98.5 mm for males, and from 83.5 to 94.8 mm for females. The mean of the rotation center (RC) of the pelvis is closer to that of the hip point (HP) for males (RC (109.2, 88.4) vs. HP (121.0, 88.4)) compared to females (RC (115.2, 35.0) vs. HP (144.0, 83.5)). This finding implies that the pelvis rotated around the hip point for males.

The average rotation center of the pelvis is lower in the *z*-position for females (35 mm) compared to males (88.4 mm). These heights of the rotation center were significantly different between males and females

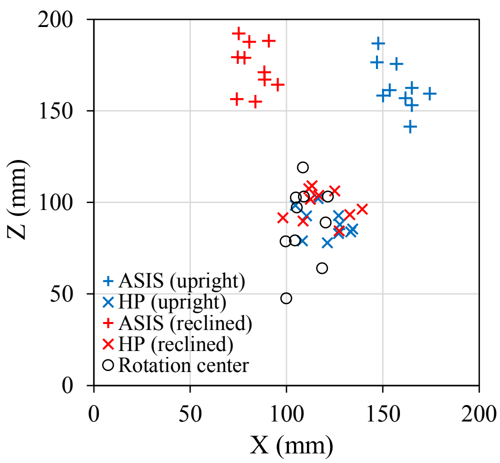

(a) Male

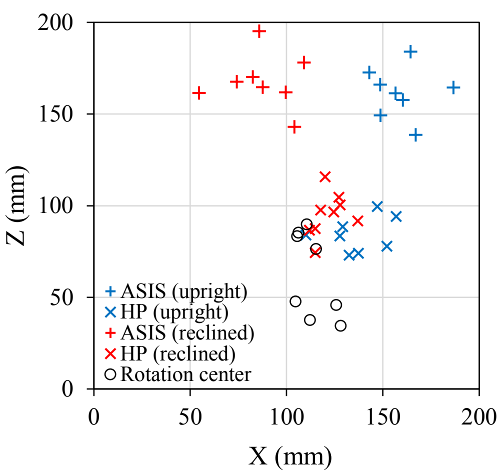

(b) Female

Fig. 15 Coordinates of the rotation center of the pelvis for changing posture from the upright sitting to the reclined sitting posture for males and females. Note that Female 16 and Female 18 are not included in this figure.

($p < 0.05$) based on the Mann-Whitney U test. In addition, as can be observed in Fig. 7, Fig. 8, and the figures in Appendix A, the contact location of the pelvis on the seat changes from the ischium in the upright sitting posture to the sacrum and the coccyx in the reclined posture, as the pelvis rotates around the hip point.

Fig. 16 shows the angle of lumbar spine for individual participants in standing, upright sitting and reclined sitting posture. The relation between the rank of lumbar spine angle by participant in the group of standing (S), upright sitting (U), and reclined sitting (R) were compared. Spearman's rank correlation coefficient was r_{SU}=0.297 ($p = 0.405$), $r_{SR} = 0.382$ ($p = 0.276$), $r_{UR} = 0.127$ ($p = 0.726$) for males, and $r_{SU} = 0.418$ ($p = 0.229$), $r_{SR} = 0.806$ ($p < 0.01$), $r_{UR} = 0.261$ ($p = 0.467$) for females. Hence, for the females, the lumbar spine angle in the standing posture by subject is related with that in the reclined posture by subject, indicating that each subject has her own lumbar lordosis angle. However, the lumbar spine angles in the upright sitting posture varied as compared to the other two postures.

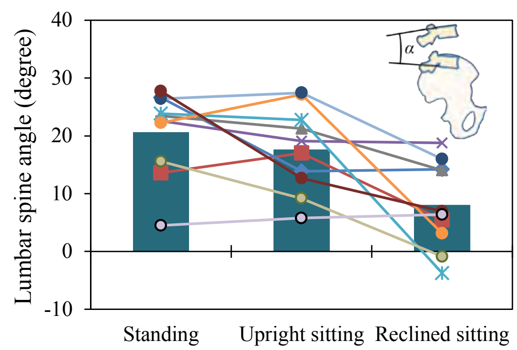

(a) Male

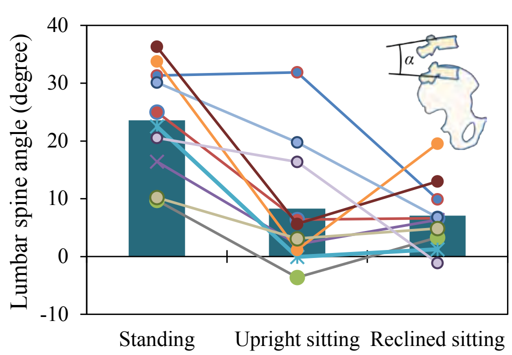

(b) Female

Fig. 16 Lumbar spine angle (L3-L5) for individual participants in standing, upright sitting and reclined sitting postures. The bars show the average.

Fig. 17 shows the relationship between the lumbar spine angle and the pelvis angle. The angle of the lumbar spine tends to decrease as the pelvis angle increases as the posture changes from standing to upright sitting to reclined sitting posture. This implies that the lumbar spine curvature changed from the S-shape to the straight-shape or the C-shape with the decrease of extension angle of the lumbar spine. The mean of lumbar spine angles in the upright sitting posture (17.6°) were comparable with the standing posture (20.7°) for males; while the mean of lumbar spine angles in the upright sitting posture (8.3°) were comparable with the reclined sitting posture (7.1°) for females.

The Soft Tissue Thickness

Fig. 18 shows the flesh margin of the ASIS in the ASIS-PSIS direction on the sagittal plane that includes the ASIS for the three postures. As the BMI increases, the ASIS flesh margin increases. In general, the flesh margin of the ASIS increases in the order from the standing posture to the reclined posture to the upright sitting posture. However, the ASIS flesh margins of Male 04 (BMI 34.2) and Male 08 (BMI 29.1) are the smallest in the upright sitting posture than in the other postures. In these subjects, a deep abdominal fold is located at the lower abdomen of the torso-thigh junction, which led to a small ASIS flesh margin. Fig. 18 also includes the ASIS flesh margin of crash dummies. The ASIS flesh margin of the Hybrid III AM50 and AF05 dummies is smaller than the participants in the upright sitting posture, while that of THOR is comparable to the participants of the same BMI level.

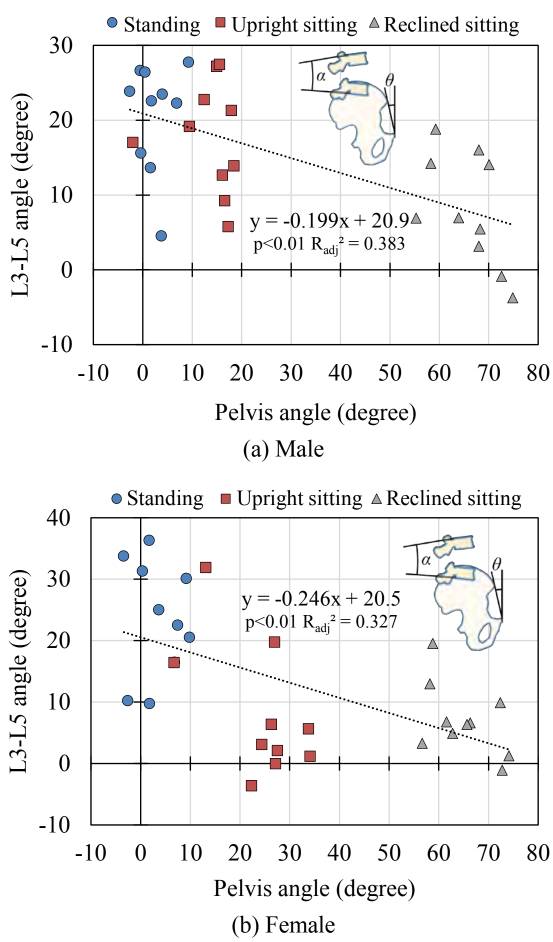

Fig. 17 Lumbar spine angle (L3-L5) vs. pelvis angle in the standing, upright sitting and reclined sitting postures for male and female

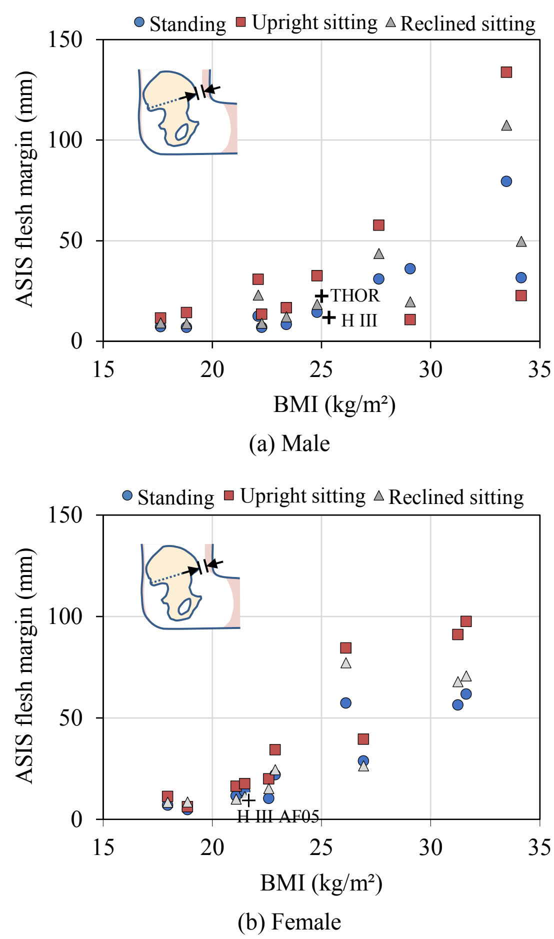

Fig. 18 The flesh margin of ASIS in the ASIS-PSIS direction on the sagittal plane across the ASIS. The data of Hybrid III AM50th, THOR AM50th and Hybrid III AF05 are included.

The abdominal fold depth at the torso-thigh junction in the upright sitting posture was measured in the x direction on the median sagittal plane for the upright sitting posture. Fig. 19 shows the relationship between this abdominal depth and the BMI. The abdominal depth is observed for males with BMI above 25 kg/m^2 and for females with BMI above 21 kg/m^2. For human subjects with BMI over 25 kg/m^2, the abdominal depth is more than 25 mm for some males and females.

The flesh margin of the great trochanter of the femur in the lateral direction is shown in Fig. 20. The flesh margin of the great trochanter increases with higher BMI. The flesh margin of the great trochanter is comparable between the upright sitting and reclined posture, and is larger than that in the standing posture. In addition, the flesh margin of the great trochanter is larger in females than in males for the same BMI; and the slope of the regression line is also larger for females than for males. From analysis of covariance, the slopes of the regression line of males and females were significantly different in standing, upright sitting and reclined sitting, respectively (p=0.0424, p=0.0083, 0.0293).

Lap belt fit with the ASIS

The overlap of the lap belt with the ASIS is shown in Fig. 21 for the upright and reclined sitting postures. The lap belt overlap is proportional to the ASIS height relative to the top of the thigh. This is because the lap belt is located at the torso-thigh junction after being worn. The overlap is affected by posture and sex. The overlap of the lap belt with the ASIS was larger for females in both upright and reclined sitting postures. From analysis of covariance, the regression lines of males and females are not significantly different in the upright sitting posture as shown in Fig. 21(a), while they are significantly different in the reclined posture ($p < 0.01$) as shown in Fig. 21(b). In the upright sitting posture, the lap belt overlapped the ASIS ($z > 0$) for 6 males and 9 females. There are two males with a negative ASIS-thigh height but also with a positive lap belt overlap. These two males (Male 02 and Male 08, see Appendix A) have the abdominal fold, and the lap belt is fitted forward and low position with respect to the deepest point of the abdominal fold. On the other hand, in the reclined posture, the lap belt did not overlap the ASIS ($z < 0$), except for only one female.

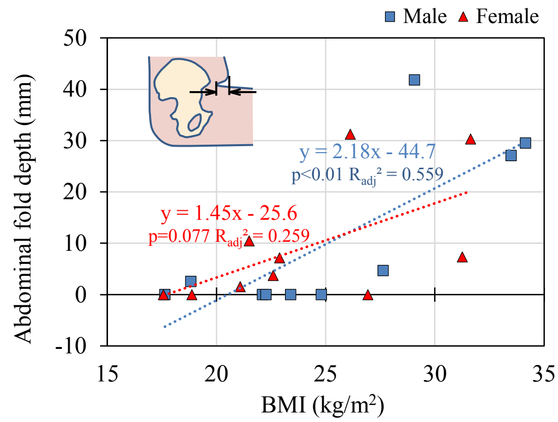

Fig. 19 The depth of the abdominal fold at the torso/thigh junction measured in the x direction on the median sagittal plane in the upright sitting posture

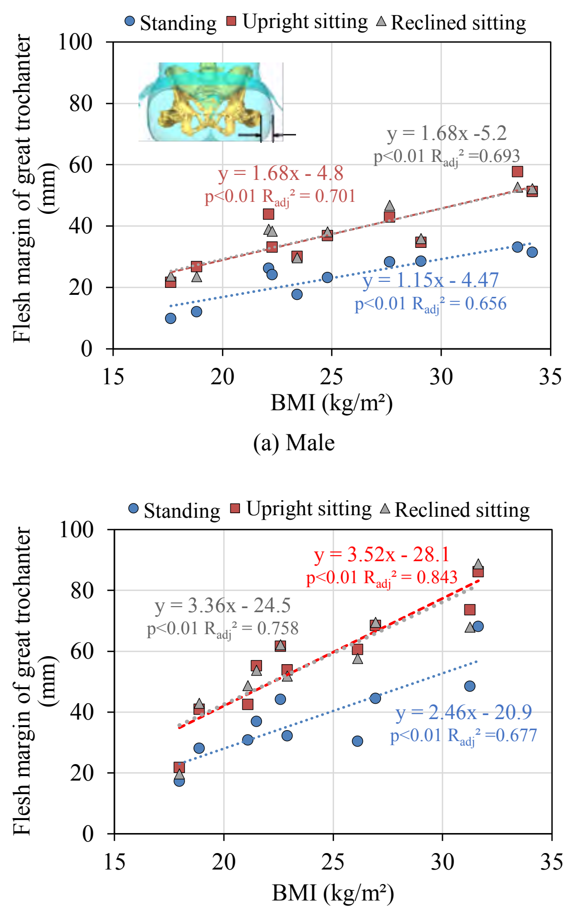

(b) Female

Fig. 20 The flesh margin of the great trochanter in lateral direction (y) in standing, upright sitting and reclined sitting posture for male and female

Fig. 22 shows the position of the lower edge of the lap belt relative to the ASIS. In the upright sitting posture, the lap belt is located in the forward direction of the ASIS. The lower edge of the lap belt is located lower than the ASIS in many participants in this sitting position. For the Hybrid III, the lower edge of the lap belt is located close in the front direction but is significantly lower with respect to the ASIS, which implies that the lap belt fully overlaps the ASIS (Fig. 9). The geometrical relation between the lap belt and the ASIS of THOR is closer to human subjects compared to Hybrid III AM50 and AF05. In the reclined sitting posture, the lower edge of the lap belt is located closer to the front and higher than the ASIS.

In the multiple regression analysis, the lap belt/ASIS overlap (z) and Lap Belt X in the upright sitting posture is expressed by sex (male 0, female 1), standing height (H), BMI and pelvis angle (PA) as:

$$\textit{Lapbelt-ASIS overlap}\ (\text{mm}) = 15.52\ \textit{sex} + 1.654\ H - 0.781\ \textit{BMI} - 1.034\ \textit{PA} - 276.0 \quad (p < 0.001,\ R_{adj}^2 = 0.605) \tag{2}$$

$$\textit{Lap Belt X}\ (\text{mm}) = 5.754\ \textit{BMI} - 49.4 \quad (p < 0.001,\ R_{adj}^2 = 0.642) \tag{3}$$

All of the above explanatory variables were significant ($p < 0.05$). For LapBelt X, the BMI was the only significant variable, and it increases as the BMI is higher.

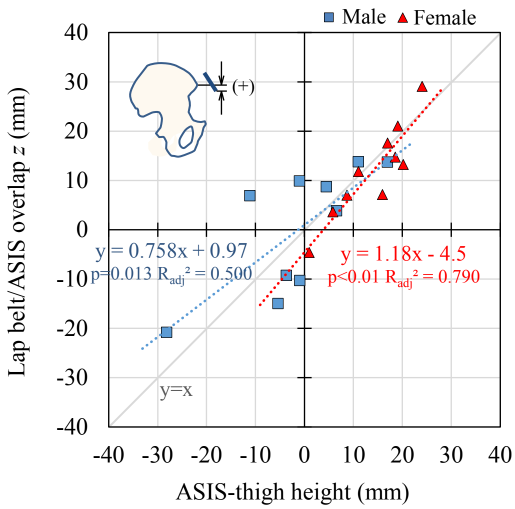

(a) Upright sitting posture

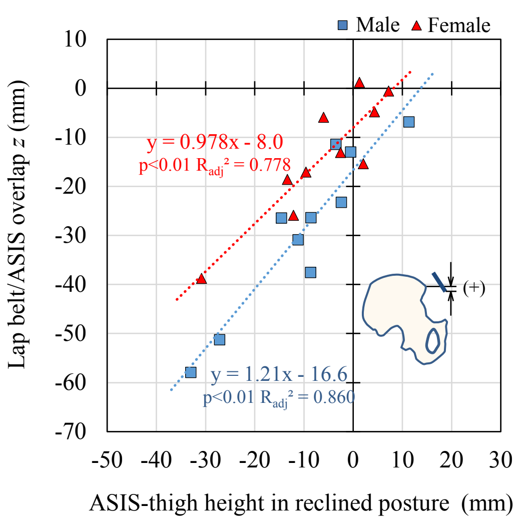

(b) Reclined sitting posture

Fig. 21 The overlap of the lap belt with the ASIS (position (z) of the lap belt lower edge relative to the ASIS) vs. the ASIS-femur top height in upright and reclined sitting posture

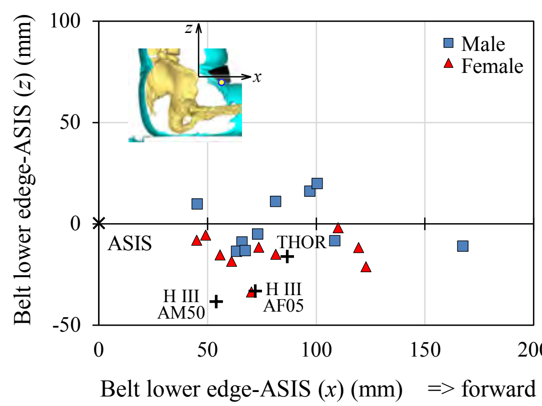

(a) Upright sitting posture

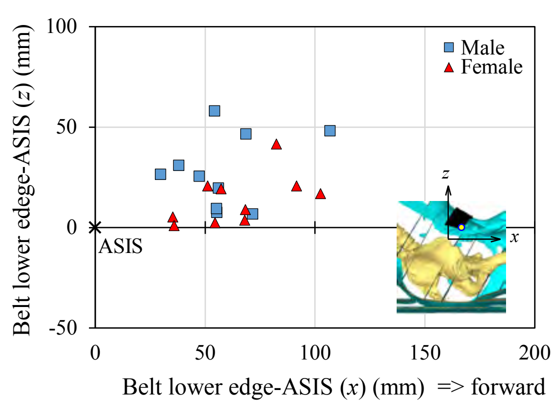

(b) Reclined sitting posture

Fig. 22 The position of the lower edge of the lap belt relative to the ASIS at the sagittal plane which goes through the ASIS in upright and reclined sitting posture

The lap belt/ASIS overlap (z) in the reclined posture (Fig. 21(b)) was expressed using sex, the ASIS-thigh height (mm), and ASIS flesh margin (mm) measured in the ASIS-PSIS direction projected on the sagittal plane in the upright sitting posture as:

$$\begin{aligned} &\textit{Lapbelt-ASIS overlap}_{\mathrm{reclined}}\ (\mathrm{mm}) \\ &\quad = 0.897\ \textit{ASIS-thigh height}_{\mathrm{upright}} \\ &\quad - 0.226\ \textit{ASIS flesh margin}_{\mathrm{upright}} - 18.4 \\ &\qquad (p < 0.001,\ R_{adj}^2 = 0.819) \qquad (4) \end{aligned}$$

All of the above explanatory variables were significant ($p < 0.05$) while sex was excluded during the calculation process because it was not a significant variable. Eq. (4) indicates that the lap belt-ASIS overlap in the reclined posture can be predicted from the variables in the upright sitting posture. The flesh margin of the ASIS has a negative effect on the lap belt-ASIS overlap because the lap belt moves upward on the abdomen in the reclined posture (see Fig. 22(b)).

The position of the lap belt and the ASIS is plotted with the abdomen outer surface around the torso/thigh junction at the ASIS sagittal plane for males and females as shown in Fig. 23 and Fig. 24, respectively. Three graphs are plotted separately for participants with low, middle, and high BMI group. The ASIS position is higher in high BMI subjects, whereas the forward position of the ASIS is comparable, irrespective of BMI. Fig. 23 and Fig. 24 also indicate that the lap belt fit location on the abdomen is similar in the upright sitting and the reclined sitting posture (the lap belt is located at the torso/thigh junction). The location of the lower edge of the lap belt relative to the ASIS is higher and the lap belt overlap of the ASIS is smaller in the reclined posture than in the upright sitting posture; and the angle of the lap belt cross section in the sagittal plane is shallower.

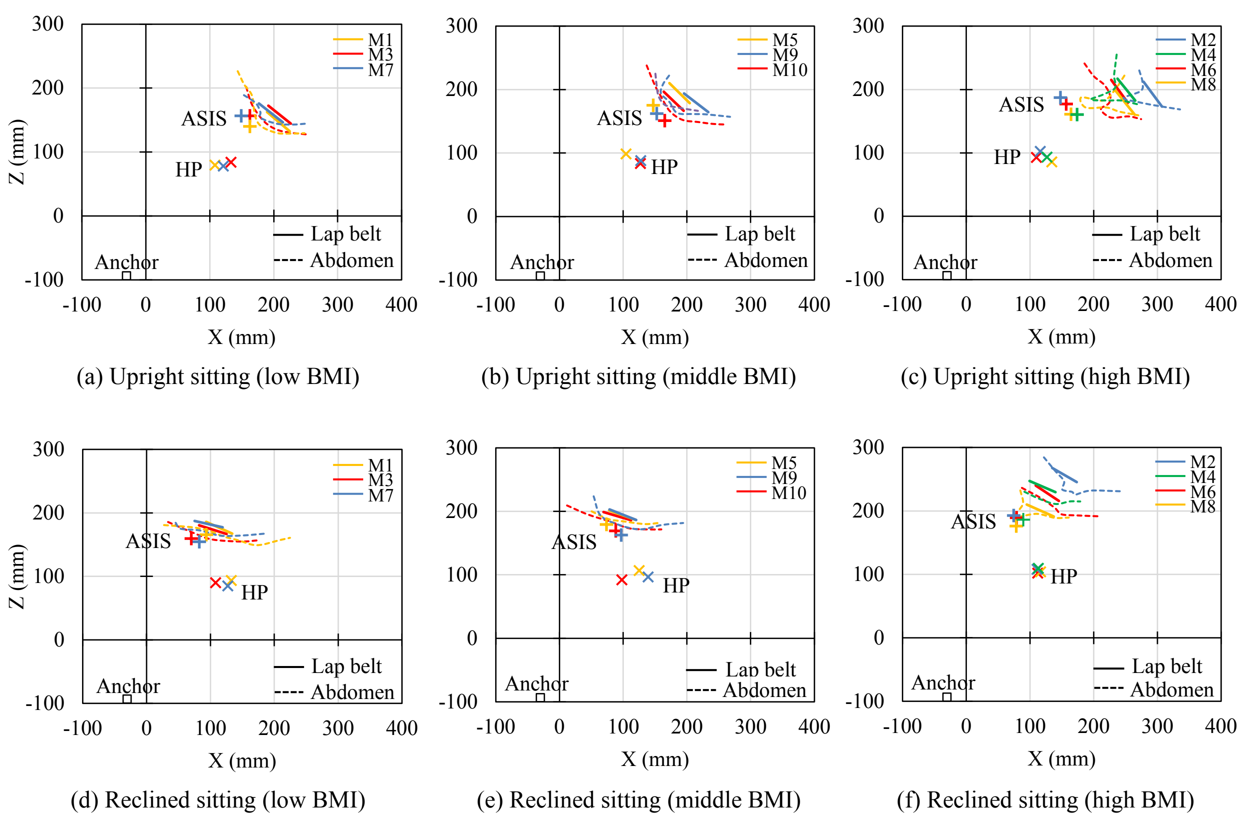

Fig. 23 The position of lap belt, outer surface around torso/thigh junction, ASIS (in the sagittal plane on the ASIS) and HP (center of acetabulum) for low, middle and high BMI participants (male).

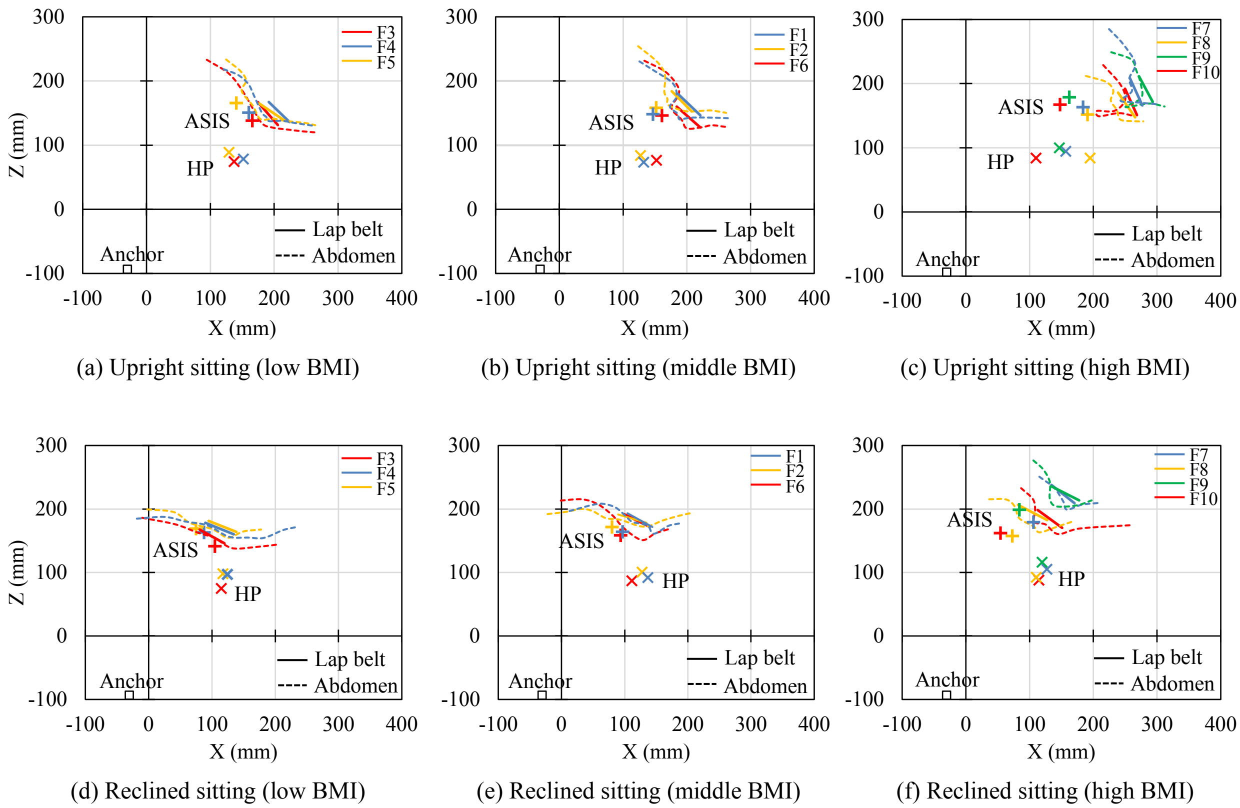

Fig. 24 The position of lap belt, outer surface around torso/thigh junction, ASIS (in the sagittal plane on the ASIS) and HP (center of acetabulum) for low, middle and high BMI participants (female).

DISCUSSION

CT Image

In many studies, the outer surfaces of human subjects have been measured using a 3D-digitizer, laser scanner, and structured light 3D scanner to investigate the seat belt fit on the pelvis. Bones and soft tissues have been imaged using X-rays, CT scanners, and MRIs. Reed et al. (2012, 2015, 2019) investigated the lap belt location relative to the ASIS using a 3D-digitizer and laser scans. In a study by Beillas et al. (2009), the thorax and the abdomen were imaged for nine participants in seated, standing, forward-flexed, and supine postures using a positional MRI. They showed that the positional MRI was effective for measuring the shape of internal organs and bones of human subjects in various postures while they focused on the shape changes of abdominal organs from the changing of postures. In our study, the geometrical relations between the bone and the soft tissue were investigated for human subjects in standing and upright sitting postures using a newly developed upright CT scan system. The lap belt path is dependent on the abdomen and thigh shape, and the lap belt path around the pelvis needs to be examined in a sitting posture. Using the upright CT scan systems, the 3D shapes of various objects could be obtained, such as the pelvic bone and abdomen with its valleys and protruding convexity of human subjects, as well as the lap belt in the upright sitting posture.

Seat Setting

The participants were seated and wore a lap belt in an upright sitting posture in the upright CT system. Due to the limited cylinder size of the upright CT scan systems, a slightly reclined sitting posture of a car occupant could not be set up. Even in the upright sitting posture, the distal region of the thigh (knee) was not included in the scan area (see Fig. 5). The angle of the driver seat of trucks and buses is upright. In these vehicles, the results of the lap belt fit in the upright sitting postures will be able to be used. However, in general, car seats have an angle, and therefore car occupants are seated in an angled posture. Hence, measurement in the upright sitting posture is a major limitation of this study.

Fig. 25 shows the Hybrid III dummy seated in the upright seat and the angled seat rotated by 15° around the seat cross line. The Hybrid III was seated under gravity and the belt was fitted in each posture. The coordinates of points in the 15°-angled seat agreed with the rotational transformation from the upright sitting posture. Thus, using the coordinates of measured points in the upright sitting posture presented in the Appendix E, the positions in the angled seat can be estimated. The overlap of the lap belt with ASIS in the angled seat can be also estimated by a rotational transformation of the coordinates of the lap belt and the ASIS in the upright posture. Note that the lap belt-ASIS overlap in the reclined posture could be estimated from the ASIS-thigh height and ASIS flesh margin in the upright sitting posture (see Eq. (4)). This result shows that the lap-belt overlap in the seat with various seatback angles has the relation with that in the upright sitting posture.

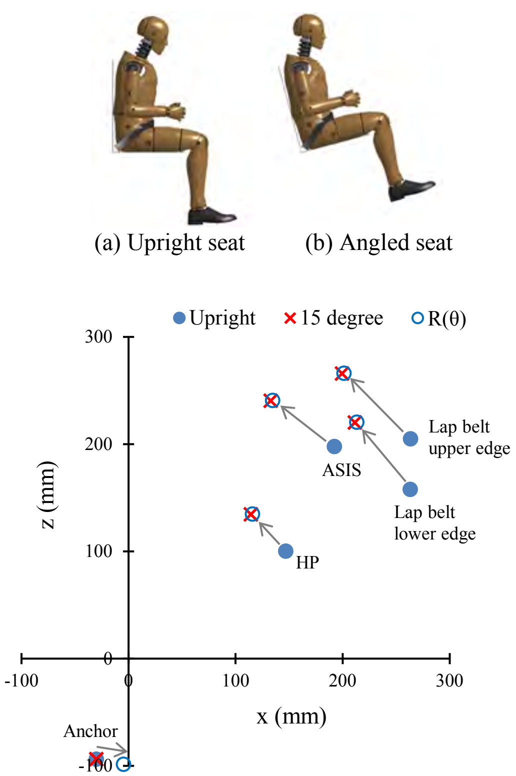

Fig. 25 The position of upright, declined, and rotational transformation R(θ) from upright to 15°-angled sitting posture. Note that the anchor point is the same for the upright and the angled seat.

Anthropometry

The outer shape of the abdomen was shown to have changed according to the standing, upright sitting, or reclined sitting postures. The soft tissues of the abdomen gathered around the torso-thigh junction according to the flexion of the hip joint. Thus, the anterior-posterior depth of the lower abdomen is larger in the sitting posture than in the standing posture. In the upright sitting posture, valleys and protruded convexity are formed in the abdomen according to the flexion of the hip joint. The soft tissue around the buttocks moves to the lateral location around the great trochanter of the femur in the sitting posture. The thigh shape changes from the standing to a sitting posture. In the front view, the shape of the cross-section of the females' thigh is triangular, widening laterally toward the seat surface (see Appendix A). This is probably because the thigh of females includes more adipose tissues around the muscle tissues and are less-stiff compared to males (adipose is shown in gray color in Appendix A).

The soft tissue thickness such as the flesh margin of the ASIS is difficult to determine from the outer surface using coordinate digitizers. Reed et al. (2012) developed a regression curve to estimate the position of the ASIS from the coordinates of the flesh outer surface at the ASIS location. They applied the flesh margin of the ASIS in the driving posture to the reclined sitting posture (Reed et al. 2019). It may be necessary to consider the effect of posture to estimate the flesh margin since the flesh margin of the ASIS changes depending on the change in the abdomen shape from the posture changes (Fig. 18). The flesh margin of the great trochanter is also larger in the sitting posture than in the standing posture (Fig. 20). Robinovitch et al. (1995) examined the attenuation effect of the trochanteric soft tissue on the risk of hip femur fractures from a fall. A pendulum (44 kg, 2.5 m/s) was impacted on trochanteric soft tissues taken from cadavers attached on a surrogate pelvis. They showed that the peak force of the pelvis decreased by 71 N for each 1 mm of increase of tissue thickness. Hence, the pelvis force exerted on pedestrians in standing postures with small flesh margin might be larger than that of vehicle occupants with large flesh margin subjected to side impacts when an external force with the same magnitude is applied around the great trochanter.

On the abdominal surface of the participants, two valleys were observed in the sagittal plane through the ASIS; the upper one at the position of the elastic strap of the pants and the lower one at the junction of the torso and thighs. In the upright sitting posture of the high BMI subjects, the convexity of the anterior abdomen is noticeable between these two valleys. The position of the trouser strings was higher in female. Participants were likely to wear the trouser belt in the same position as the elastic strap of the trousers used in this study. Thus, the shape of the abdomen in the upright sitting posture will represent the shape of the abdomen while sitting on the seat in the car.

The relatively deep abdominal fold (deep valley) at the torso/thigh junction was observed for high BMI participants (Male 04 and Male 08). These participants put the trouser elastic cord at this location, which could lead to a deeper fold. This deep abdominal fold resulted in the close distance between the deepest point of the abdominal fold and the ASIS. The lap belt was located around the opening of the abdominal fold as shown in Appendix A. Lebarbé et al. (2020) examined the geometrical shape and the mechanical characteristics of the abdominal fold for extremely high BMI PMHS from CT image, lap belt pulling tests, and sled tests. In their sled tests, the lap belt slipped into the abdominal fold and engaged the ASIS. The abdominal fold would not have generated any resistance force to the lap belt until the lap belt moved into the deepest point of the abdominal fold. Hence, the abdominal fold would have contributed slack to the seat belt. In addition, the abdominal fold opened in the reclined posture for Male 08 (see Fig. A8), and the lap belt fitted stably in this location.

In this study, a clear trend was not observed for the pelvis angle and the BMI (Fig. 14). This result was comparable with Izumiyama's study (2017) that the pelvis angle did not have a significant relation with the BMI. Izumiya also pointed out the pelvises of high-BMI subjects (BMI > 30 kg/m^2) have anteriorly tilted angles. However, this pelvis posture was not observed in high-BMI subjects in this study. One possible reason is the pelvis angle varies in individuals and the number of data in this study was small. Instead, in our study, the pelvis angle was observed to be tilted rearward in the order of standing, upright sitting, and reclined sitting postures (see Fig. 14). The ratio of pelvis angle change to seat back angle change was 1.16 (=(65.9°−13.7°)/(90°−45°), see Fig. 14(a)) from the upright to the reclined sitting posture. Reeds et al. (2019) developed a regression equation of the pelvis angle in the various reclined seat back angles of a car seat, and the coefficient of pelvis angle as a parameter of the seat back was 0.331. We consider that this low coefficient could be attributed to the soft seat-cushion conditions of the car front seat used in Reed's study.

The rotation center of the pelvis from the upright sitting to the reclining posture locates around the hip joint for males while it locates lower than the hip point for females. This is likely because the females tended to be seated anteriorly in the upright sitting posture. When the displacement of the pelvis includes translation in the longitudinal direction, the rotation center of the pelvis is calculated at a lower position. Note that Female 16 and 18 were not included in Fig. 15(b) because they sat anteriorly on the seat in the upright sitting posture and the vertical position of the rotation center was negative.

Because of the limitation of the supine CT scan system, the upper lumbar spine was not included in the images. Fig. 26 shows L1-L3 angles and L1-L5 angles in the standing and upright sitting postures. The correlation is observed ($R_{adj}^2 = 0.619$), and the L1-L5 angle might be estimated using this regression. The lumbar spine angle decreased with an increasing angle of the posterior pelvic tilt in the order of standing, upright sitting, and reclined sitting postures (see Fig. 17). Participants have their individual lumbar spine curvature in the standing and reclined sitting postures. This is consistent with the results of Beillas et al. (2009), who showed reproducible patterns in spinal kyphosis/lordosis and pelvic tilt angles among individuals between supine, seated, standing, and forward bending postures. In the upright sitting posture in our study, participants had a variety of lumbar lordosis and pelvic tilt angles. In addition to having used a rigid seat, these various angles in the upright sitting posture may be because the participants were not instructed on the sitting posture; and therefore sat in various pelvic positions, either tensed or relaxed.

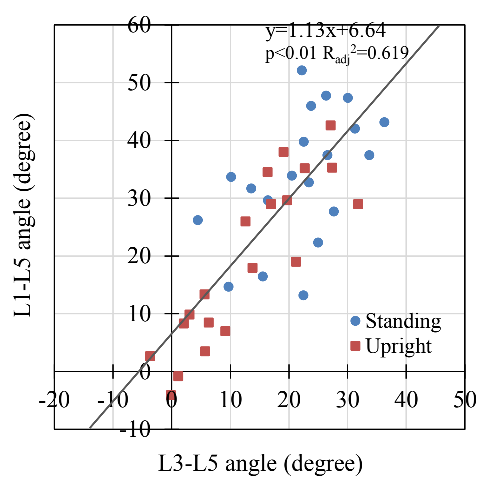

Fig. 26 The lumbar spine angle of L1-L5 and L3-L5 in the standing and the upright sitting postures.

Lap Belt Fit

It was found that the overlap of the lap belt with the ASIS was larger for females than for males in the upright sitting posture (Fig. 21(a)). The reason for this difference is mainly due to the differences in the shape of the thigh cross-section between males and females. The small anterior-posterior diameter of the thigh of females led to a large ASIS height relative to the thigh. A few studies discussed the lap belt fit by sex difference. Izumiyama et al. (2017) observed no differences in the distance from the pubic symphysis to the ASIS between males and females. LapBelt X (X coordinates of the lap belt upper edge relative to the ASIS) was formulated by Reed and Ebert (2013), and it was determined that BMI has the largest effect on the BMI while the participant's sex was not a significant factor. Similarly, in Eq. (3), LapBelt X was expressed only by BMI, and the participant's sex was not a significant factor. However, it will be necessary to include the pelvis shape and thigh and abdomen shape to discuss differences in the lap belt fit with ASIS by sex. In the reclined sitting posture, the overlap of the lap belt with the ASIS was significantly larger in females, even when the ASIS-thigh height was the same (Fig. 21(b)). This is likely because the abdominal valley located at the thigh/torso junction in the middle-high BMI females in the reclined posture, and the lap belt fitted in this valley (Fig. 24(b)).

The better overlap of a lap belt with the ASIS for females than for males is beneficial to the lap belt engagement with the ASIS in the initial stage of impacts. However, Rawska et al. (2020) conducted front impact FE simulations in changing seat back angles; and they suggested that a small female was prone to submarining compared to midsize and large males. They considered that the female's small pelvis, the buckle position, and the lap belt shallow angle contributed to submarining during impacts. They also added the lap belt position of the female as one of the factors leading to submarining because the lap belt would locate superior to the pelvis in its initial posture due to the small size pelvis. Even though the lap belt of females overlaps sufficiently with the ASIS in initial conditions, the lap belt might slip from the ASIS according to the pelvis rotation and the shallow lap belt angle during impacts due to the small size of the pelvis.

Abe et al. (2021) examined the lap belt engagement with ASIS using FE simulations in the rear seat in a frontal impact (50 km/h) in various conditions: modified THUMS (flat/protruding abdomen, large/medium thigh diameter), seat pan (flat/slant), lap belt pretensioner (with/without), and lap belt anchor location (forward /standard). In the initial phase of impact, the lap belt went over the ASIS for the human model with a flat abdomen and large thigh diameter (no initial overlap of the lap belt with ASIS) because there was not enough distance for the lap belt to catch the ASIS. Even in this case, the lap belt engaged the ASIS when the lap belt pretensioner is activated. In Fig. **23** and Fig. 24, the relation between the lap belt, the ASIS, and the anchor point may be considered in the upright sitting posture as an example (Note that the geometry of upright sitting posture is different from the standard car seat). In the initial phase of impacts when the lap belt force and the force from the seat are small, the pelvis moves in the vehicle's forward direction in the passenger compartment. As shown in Fig. 23, the lap belt may not engage the ASIS for some middle-BMI male participants if the pelvis moves forward because the lap belt is above the ASIS and the distance between the lap belt and the ASIS is small. When a lap belt pretensioner is installed and activated, the lap belt is pulled toward the anchor, and the lap belt can engage the ASIS for all participants because the ASIS locates above the line that connects the lap belt and the anchor.

In our previous study, participants sat in a rigid seat wearing a three-point seat belt with a retractor, and the lap belt path was measured statically as they moved their pelvis forward by 10 cm from an upright sitting to a slouching posture (Mizuno et al. 2019). In low BMI participants with a flat abdomen, the lap belt moved upward to the middle of the abdomen because the lap belt took the path where its length was the shortest due to belt tension from the retractor. On the other hand, in high BMI participants, the lap belt was trapped and stayed in the valley of the abdomen even when the posture changed. In this current study, in the reclined sitting posture, the abdomen shape is flat for low BMI subjects as shown in Fig. 23 and Fig. 24. Though the lap belt was initially positioned in the torso/thigh junction in the reclined posture, it is possible that the lap belt will move from the torso/thigh junction to the umbilical region of the abdomen for low-BMI occupants during riding when the pelvis is positioned forward or the lap belt anchor is positioned rearward. Even though these occupants initially placed the lap belt at the torso/thigh junction, the lap belt can move to the abdominal region because the retractor force applies a pulling force to the lap belt during car rides, which works to minimize the total lap belt length. In contrast, for high-BMI subjects, the lap belt will stay at the valley of the torso/thigh junction due to the abdominal anterior protruded convexity. Note that this shortest path of the lap belt may be different for some obese occupants who wear the lap belt on the abdomen above the torso/thigh junction (Reed et al. 2012).

Limitations

This study has limitations that the participants were measured in upright sitting and reclined sitting postures with the seat back at 45 degrees, which were different from the driving positions when sitting in an actual car seat (the seat back angle of standard driving posture is around 15-25 degrees). Hence, the overlap of the lap belt with the ASIS of vehicle occupants in real-world is likely between the upright sitting posture and the reclined sitting posture measured this study. In addition, the seat used in this study was stiff, and therefore is different from car seats with soft cushions. This stiff seat will affect the angle of the pelvis and the lumbar spine. In this study, only one geometry of the lap belt was examined; however, the overlap of the lap belt with the ASIS can vary depending on the anchor position of the lap belt. Though the abdomen shape, the amount of muscle, and the lap belt path are dependent on age (Reed et al. 2013), elderly people were not included in the participants in this study. Also, the number of participants in this study was not sufficient for analyzing the data statistically with various parameters.

CONCLUSIONS

In this study, the 3-dimensional shapes of bones and flesh around the pelvis were obtained using a CT scan for 10 male and 10 female participants wearing a lap belt. The standing and upright sitting postures were scanned by an upright CT scan system, and the reclined sitting posture was scanned by a supine CT scan system. The results are summarized as follows:

1. In the upright sitting posture, the ASIS height relative to the top of the thigh was smaller as the BMI increases. This ASIS-thigh height was statistically significantly higher for females than that for males because of the small anterior-posterior diameter of the females' thigh in a sitting posture.

2. The pelvis is tilted more rearward and the curvature of the lumbar spine is smaller in the order of the standing, upright sitting, and reclined sitting postures. The rotation center of the pelvis from the upright sitting posture to the reclined sitting posture was located around the hip joint (center of the acetabulum). In the standing and reclined sitting posture, the features of the pelvis and the lumbar spine posture of each individual were remained in females.

3. The lap belt was fitted at the torso/thigh junction in the upright sitting posture. The overlap of the lap belt with the ASIS depends on the ASIS height relative to the top of the thigh. Thus, females had a larger overlap of the lap belt with the ASIS than in males in the upright sitting and the reclined sitting postures.

4. In the abdomen of a high BMI person, two valleys are formed at the junction of the trouser strap and the torso/thighs, and an anterior convexity protrudes between the two valleys. The anterior-posterior depths of the concaves and valleys were noticeably larger in the order of the standing posture to the reclined sitting to the upright sitting postures.

5. The lap belt location on the abdomen is similar in the upright and the reclined sitting posture. However, in the reclined sitting posture, the lap belt is located upward relative to the ASIS, and the overlap of the lap belt with the ASIS decreased due to rotation of the pelvis.

REFERENCES

Abe, H., Mizuno, K., Tanaka, Y. 2021. Studies of the interaction between the lap belt and anterior superior iliac spine. Transactions of Society of Automotive Engineers of Japan, 52(2) 337-342 (in Japanese).

Beillas, P., Lafon, Y., Smith, F. W. 2009. The effects of posture and subject-to-subject variations on the position, shape and volume of abdominal and thoracic organs. Stapp Car Crash Journal, 53, 127-154.

Horsch, J.D., Hering, W.E. 1989. A kinematic analysis of lap-belt submarining for test dummies. Proc. 33rd Stapp Car Crash Conference, 281-288.

Izumiyama, T., Nishida, N., Iwanaga, H., Chen, X., Ohgi, J., Asahi, R., Fukushima, M. 2020. Identification of influential factors for seatbelt kinematics in a collision and analysis of their influence degree to the kinematics. IRCOBI conference.

Izumiyama, T., Nishida, N., Iwanaga, H., Chen, X., Ohgi, J., Asahi, R., Fukushima, M. 2019. Analysis of individual differences in pelvic shape and its impact on the seatbelt kinematics in a collision. IRCOBI conference.

Izumiyama, T., Nishida, N., Iwanaga, H., Chen, X., Ohgi, J., Mori, K., Ueno, M. 2018. The analysis of an individual difference in human skeletal alignment in seated posture and occupant behavior using HBMs. IRCOBI conference.

Jinzaki M., Yamada Y., Nagura T., Nakahara T., Yokoyama Y., Narita K., Ogihara N., Yamada M. 2020. Development of upright computed tomography with area detector for whole-body scans: phantom study, efficacy on workflow, effect of gravity on human body, and potential clinical impact. Investigative Radiology, 55(2) 73-83.

Kahle W., Leonhardt H., Platzer W. 1986. Color atlas/text of human anatomy, Vol.1 Locomotor system, 3rd revised edition. Thieme Inc.

Kahane, C. 2000. Fatality reduction by safety belts for front-seat occupants of cars and light trucks. Technical Report. DOT HS 809 199. National Highway Traffic Safety Administration.

Kent, R.W., Forman, J.L., Bostrom, O. 2010. Is there really a “cushion effect”?: A biomechanical investigation of crash injury mechanisms in the obese. Obesity, 18(4), 749-753.

Lamielle, S., Cuny, S., Foret-Bruno, J.Y., Petit P., Vezin P., Verriest, J.P., Guillemot, H. 2006. Abdominal injury patterns in real frontal crashes: Influence of crash conditions, occupant seat and restraint systems. Annu Proc Assoc Adv Automot Med 50:109–124.

Lebarbé, M., Beillas, P., Janak, T., Lafon, Y., Richard, O., Petit, P. (2020). Geometrical and mechanical characterization of the abdominal fold of obese post mortem human subjects for use in human body modelling. Stapp Car Crash Journal, 64, 213-267.

Leung, Y.C., Tarrière, C., Fayon A., Mairesse P., Banzet P. 1981. An anti-submarining scale determined from theoretical and experimental studies using three-dimensional geometrical definition of the lap-belt. Proc. 25th Stapp Car Crash Conference, 685-729.

Leung, Y.C., Tarrière, C., Lestrelin, D., Hureau, J., Got, C., Guillon, F., Patel, A. 1982. Submarining injuries of 3 pt. belted occupants in frontal collisions – description, mechanisms and protection. SAE paper 821158, 26th Stapp Car Crash Conference.

Lin, H., Gepner, B., Wu, T., Forman, J., Panzer, M. 2018. Effect of seatback recline on occupant model response in frontal crashes. IRCOBI Conference.

Mizuno, K., Hatano, W., Yoshida, R., Nakajima, Y., Tanaka, Y., Muroya, T., Ishigaki, R. 2019. The geometrical relationship between the lap belt and occupants'anterior superior iliac spine. In 26th International Technical Conference on the Enhanced Safety of Vehicles (ESV).

Mizuno, K., Yoshida, R., Nakajima, Y., Tanaka, Y., Ishigaki, R., Hosokawa, N., Hitosugi, M. 2018. The effects of inboard shoulder belt and lap belt loadings on chest deflection. Stapp Car Crash Journal, 62, 67-91.

Östling M., Sunnevång C, Svensson C., Kock H.O. 2017. Potential Future Seating Positions and the Impact on Injury Risks in a Learning Intelligent Vehicle (LIV). VDI-Tagung Fahrzeugsicherheit, Berlin, Germany.

Park, J., Ebert, S.M., Reed, M.P., Hallman, J.J. 2018. Comparison of three-point belt fit between humans and ATDs in rear seats. Traffic Injury Prevention, 19(sup1), S65-S69.

Rawska K., Gepner B., Kulkarni S., Chastain K., Zhu J., Richardson R., Perez-Rapela D., Forman J., Kerrigan J. 2019. Submarining sensitivity across varied anthropometry in anautonomous driving system environment. Traffic Injury Prevention, 20(sup2), S123-S127.

Rawska, K., Gepner, B., Moreau D., Kerrigan J. 2020. Submarining sensitivity across varied seat configurations in autonomous driving system environment. Traffic Injury Prevention, 21(sup1), S1-S6.

Reed, M.P., Ebert-Hamilton, S.M., Rupp, J.D. 2012. Effects of obesity on seat belt fit. Traffic Injury Prevention, 13(4), 364-372.

Reed, M.P., Park, B.K., Hallman, J.J. 2015. Effects of driver attributes on lower abdomen contour. IRCOBI conference.

Reed, M.P., Ebert, S.M., Jones M.L.H. 2019. Posture and belt fit in reclined passenger seats. Traffic Injury Prevention, 20(sup1), S38-S42.

Richardson, R., Donlon, J.P., Jayathirtha, M., Forman, J.L., Shaw, G., Östling, M., Pipkorn, B. 2020. Kinematic and injury response of reclined PMHS in frontal impacts. Stapp Car Crash Journal, 64, 83-153.

Robinovitch, S., McMahon, T., Hayes, W. 1995. Force attenuation in trochanteric soft tissues during impact from a fall. Journal of Orthopaedic Research, 13(6), 956-962.

Rouhana, S.W., Horsch, J.D., Kroell, C. 1989. Assessment of lap-shoulder belt restraint performance in laboratory testing. SAE paper 892439, 33rd Stapp Car Crash Conference.

Wells, R.P., Norman, R.W., Bishop, P., Ranney, D.A. 1986. Assessment of the static fit of automobile lap-belt systems on front-seat passengers. Ergonomics 29(8), 955-976.

APPENDIX A

CT images of standing, upright sitting (center, sagittal plane and the transverse plane that goes through the ASIS, front) and reclined sitting posture are shown in figures. In the cross-section figures, muscles are shown in green, others in gray, and the lap belt in blue.

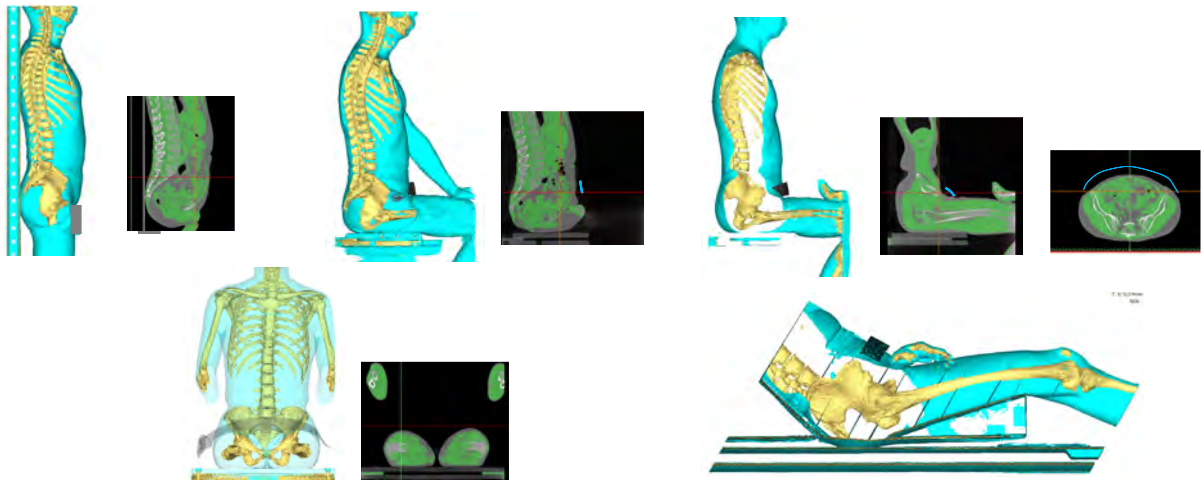

Fig. A1 Male 01 (BMI 18.8)

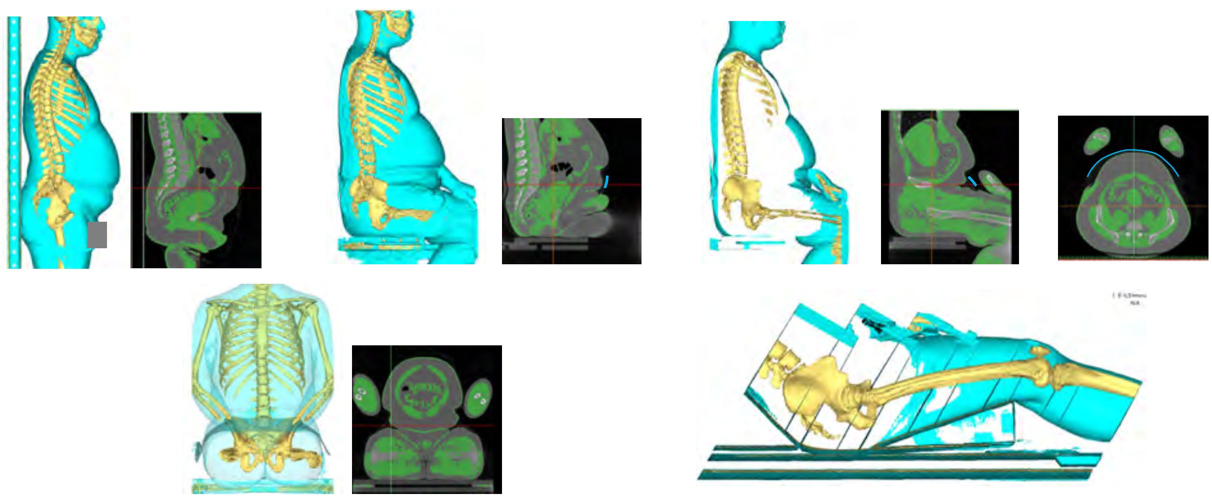

Fig. A2 Male 02 (BMI 33.5)

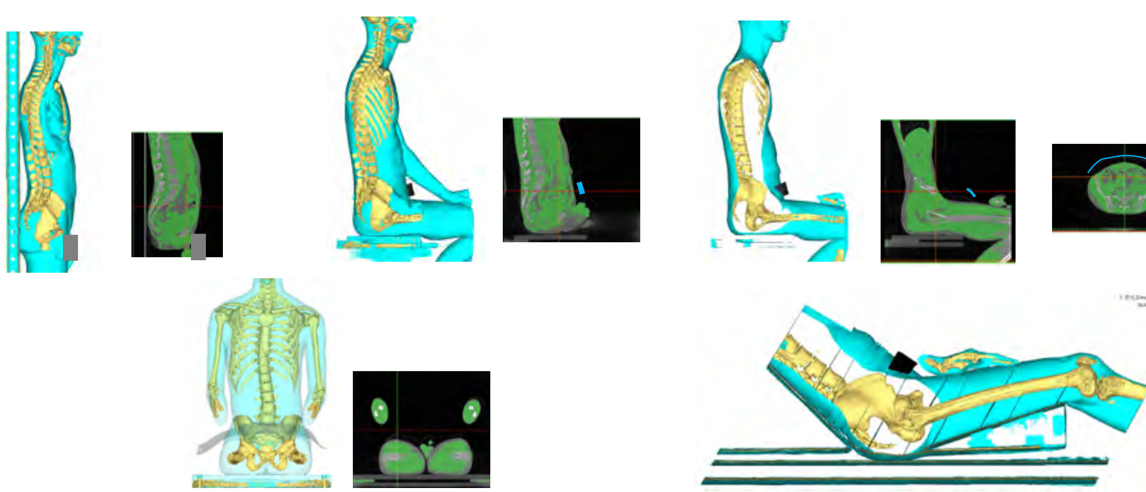

Fig. A3 Male 03 (BMI 17.6)

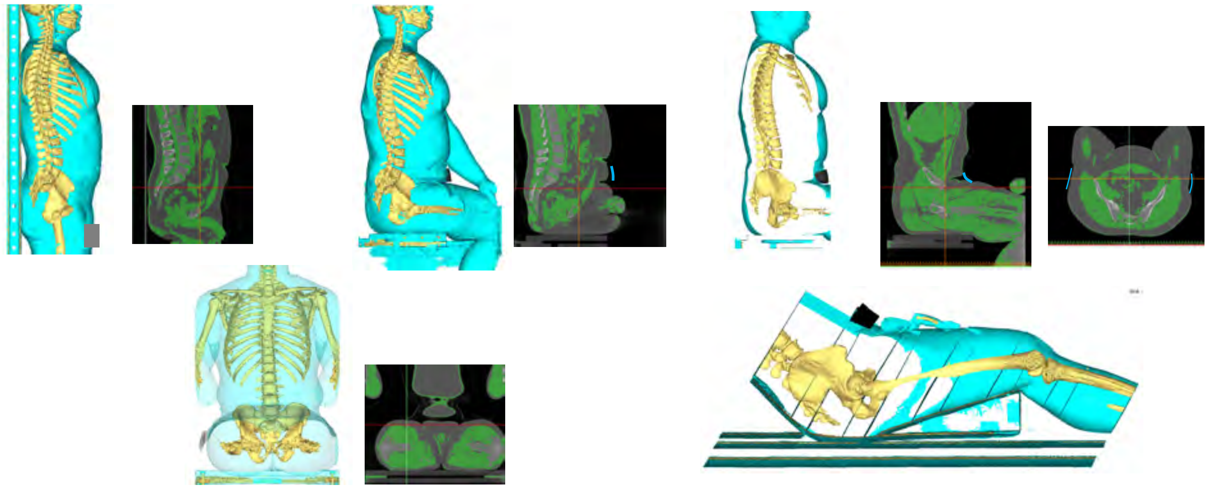

Fig. A4 Male 04 (BMI 34.2)

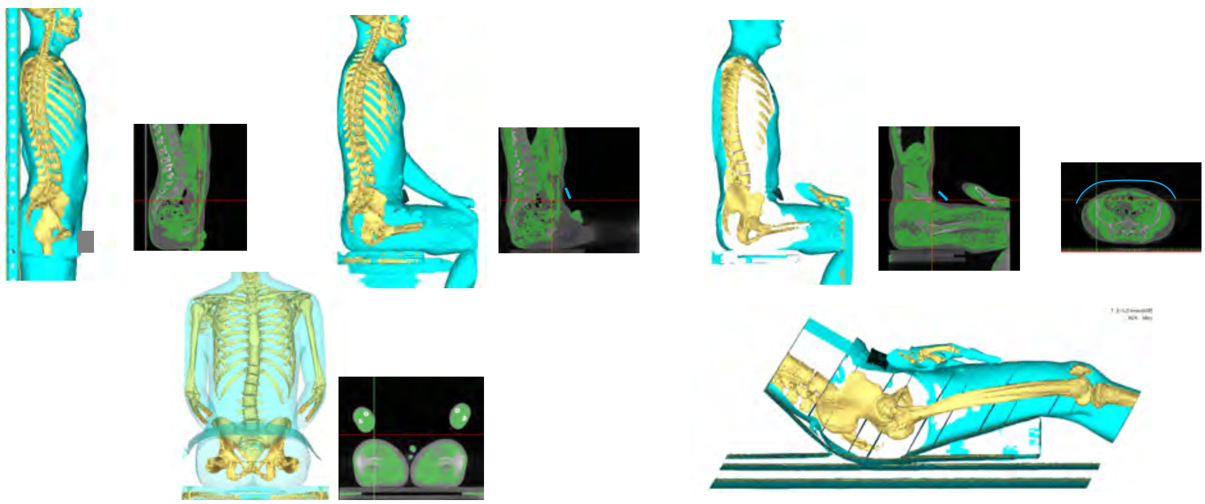

Fig. A5 Male 05 (BMI 23.4)

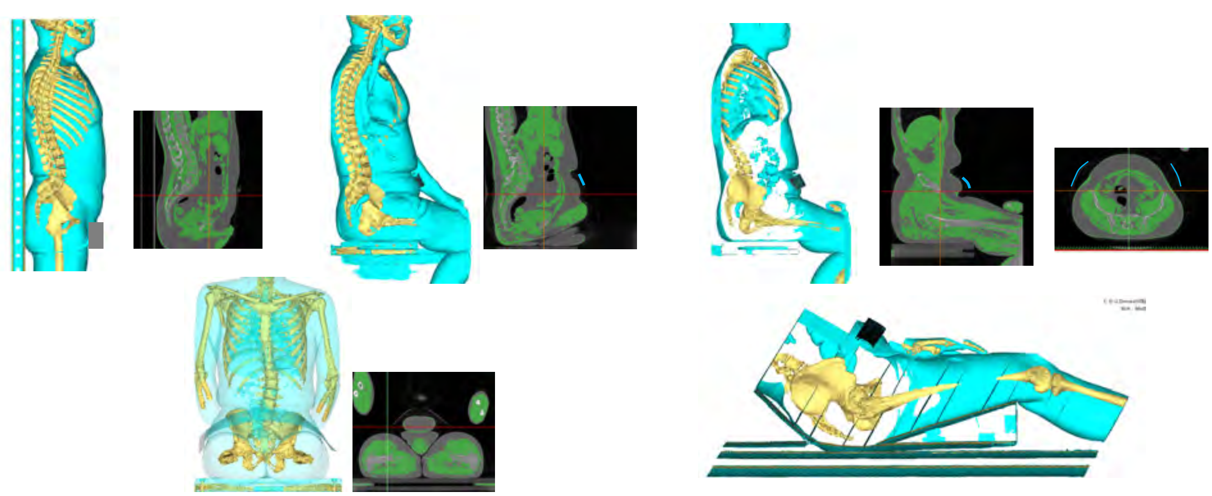

Fig. A6 Male 06 (BMI 27.6)

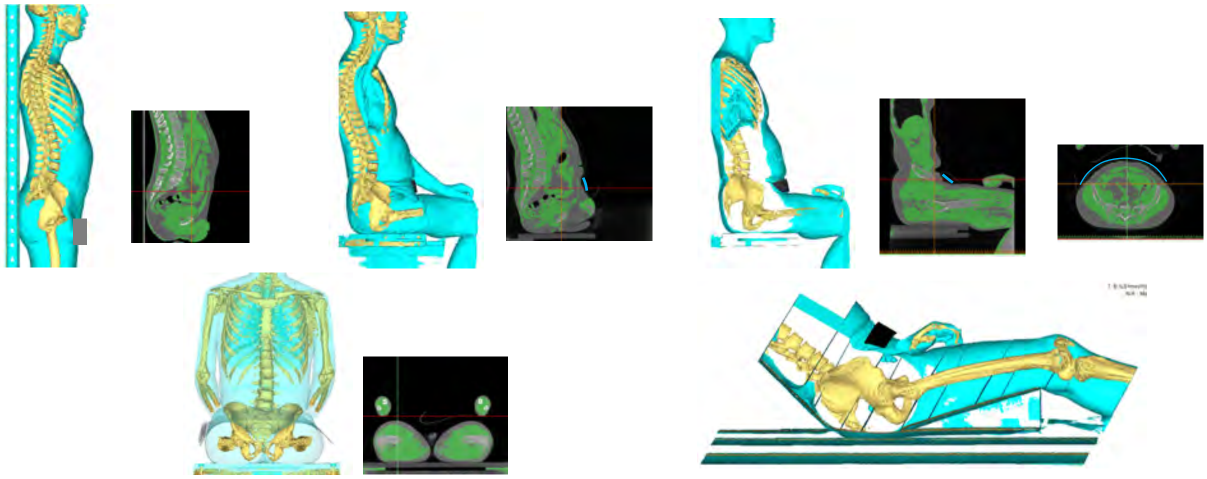

Fig. A7 Male 07 (BMI 22.1)

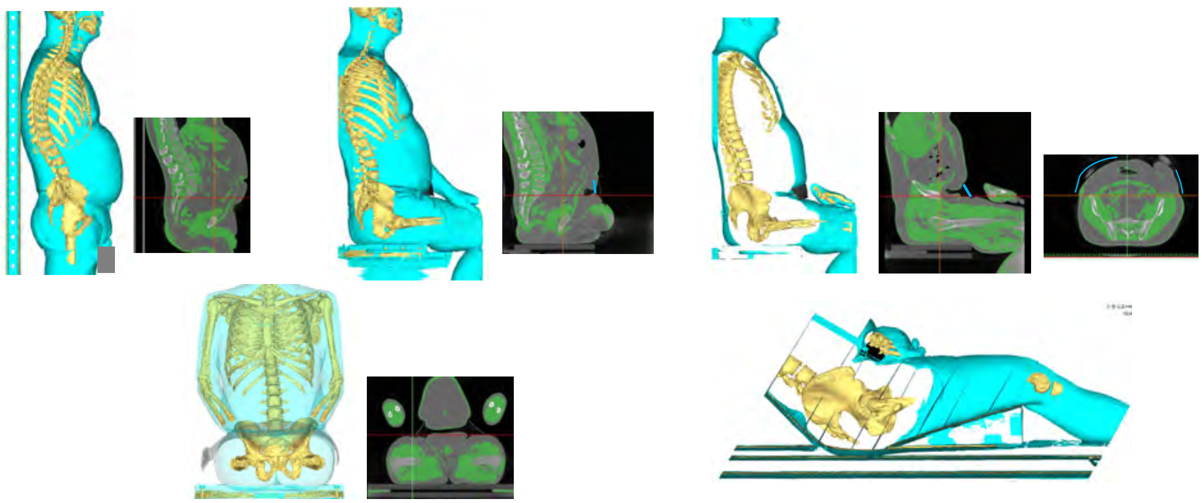

Fig. A8 Male 08 (BMI 29.1)

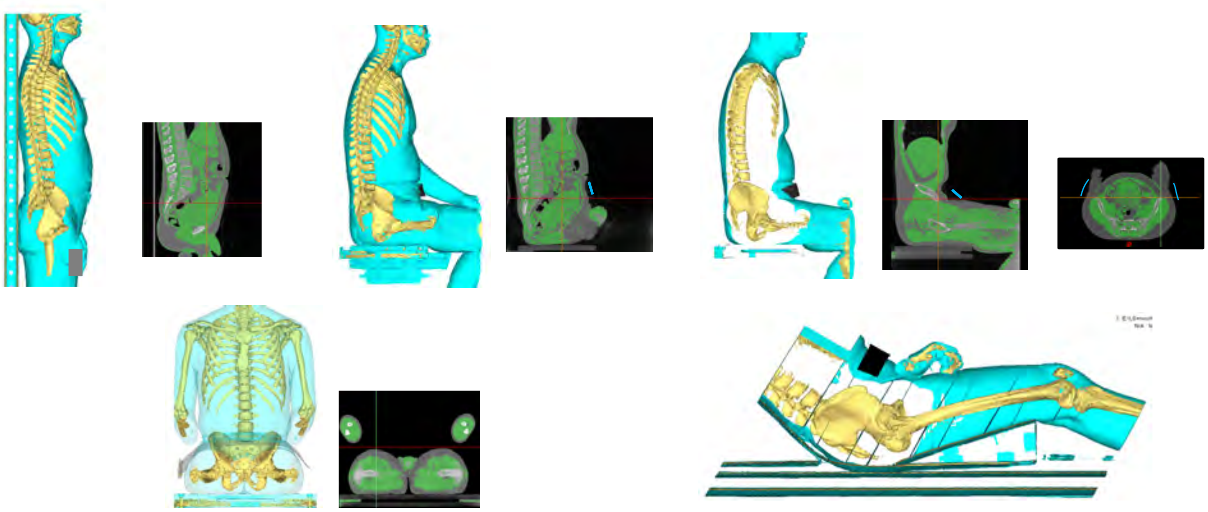

Fig. A9 Male 09 (BMI 24.8)

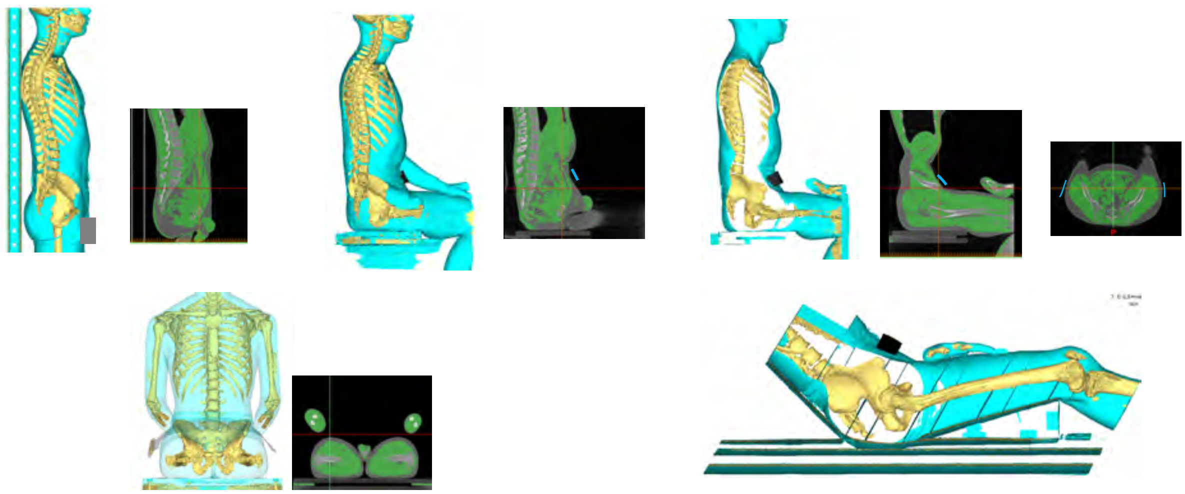

Fig. A10 Male 10 (BMI 22.3)

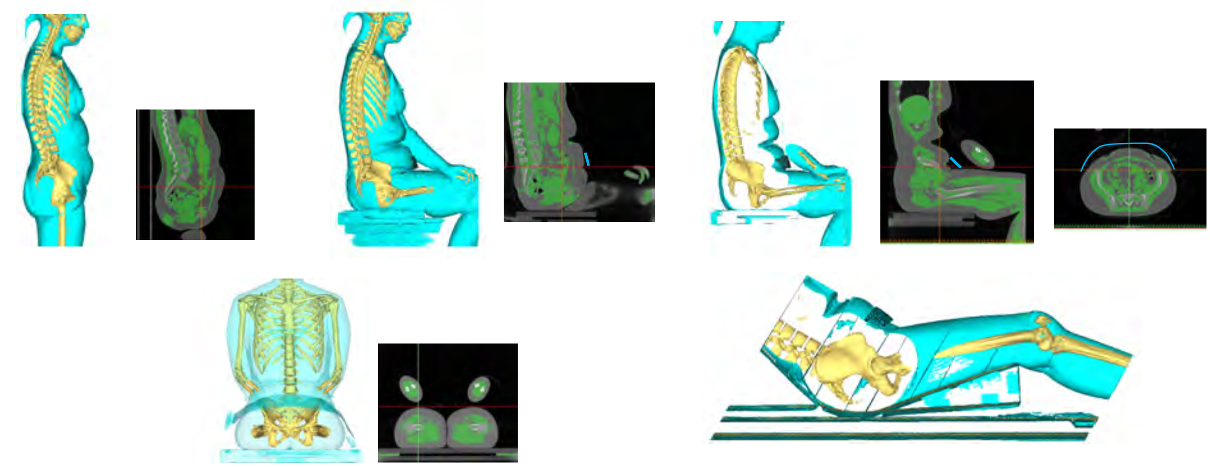

Fig. A11 Female 01 (BMI 22.9)

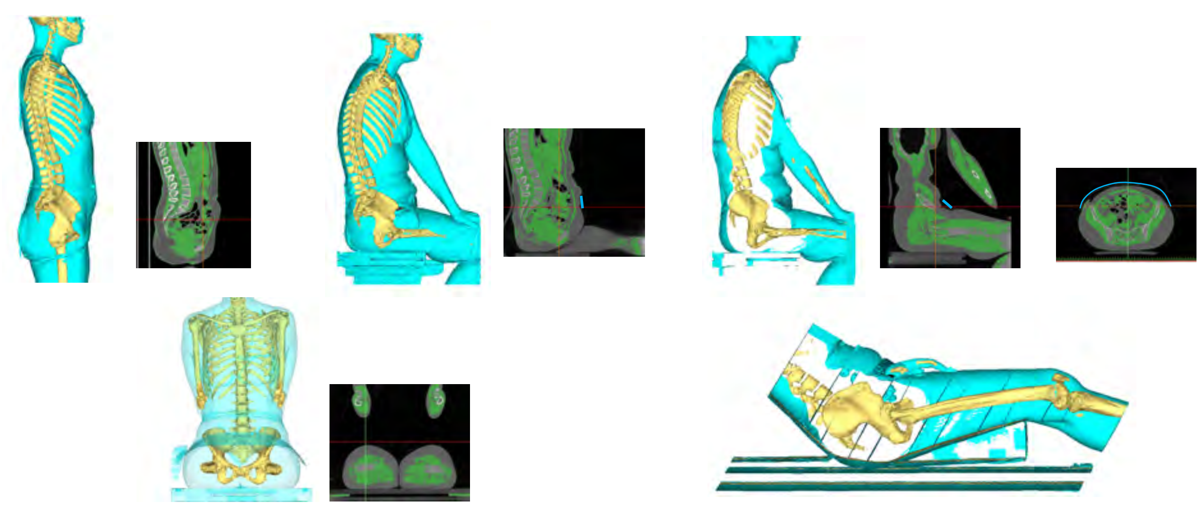

Fig. A12 Female 02 (BMI 22.6)

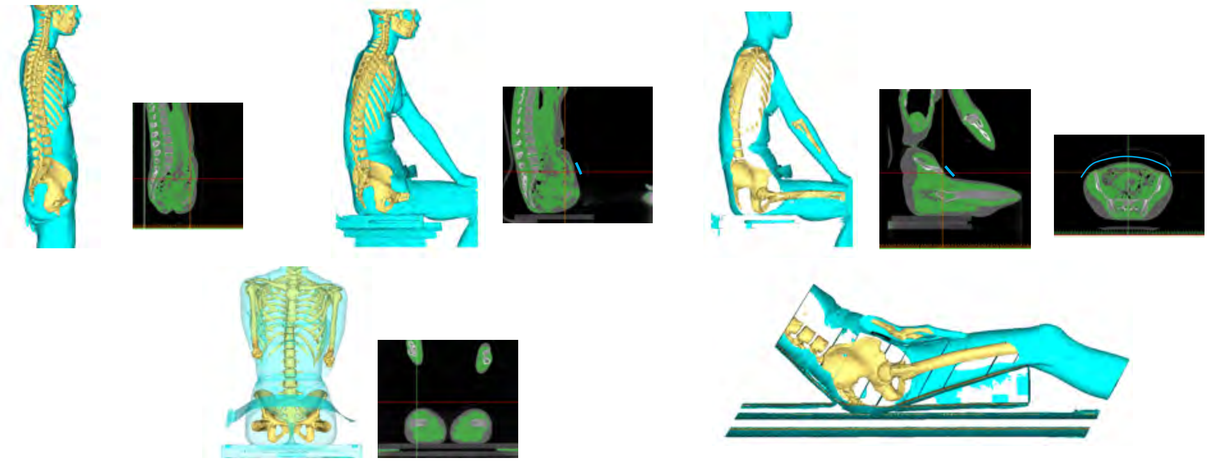

Fig. A13 Female 03 (BMI 17.6)

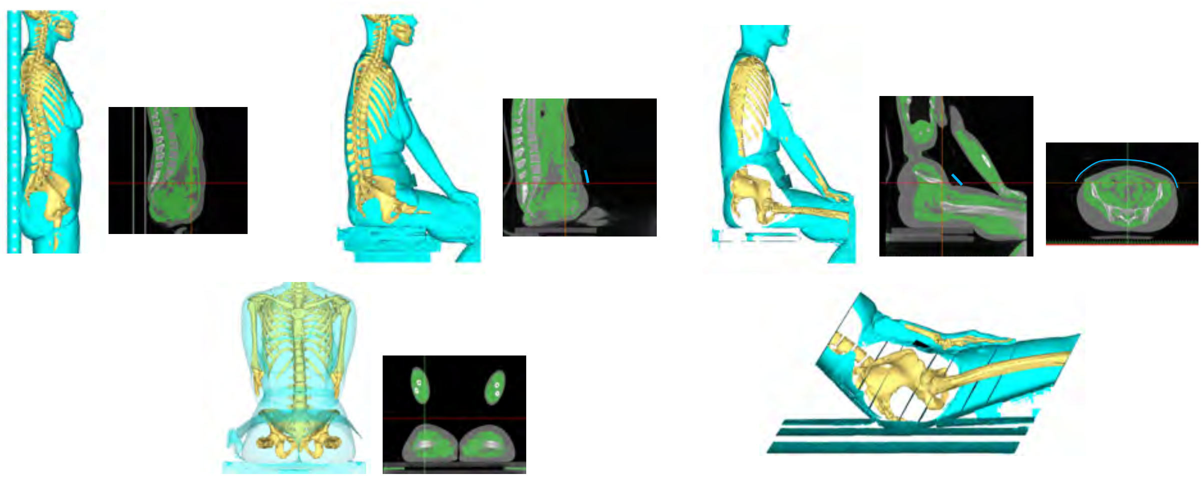

Fig. A14 Female 04 (BMI 21.1)

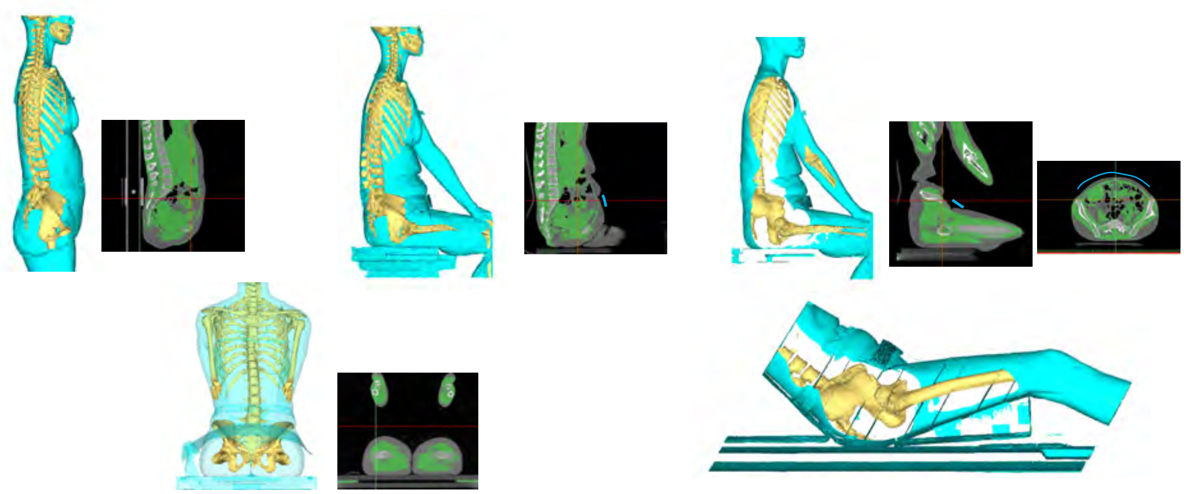

Fig. A15 Female 05 (BMI 18.9)

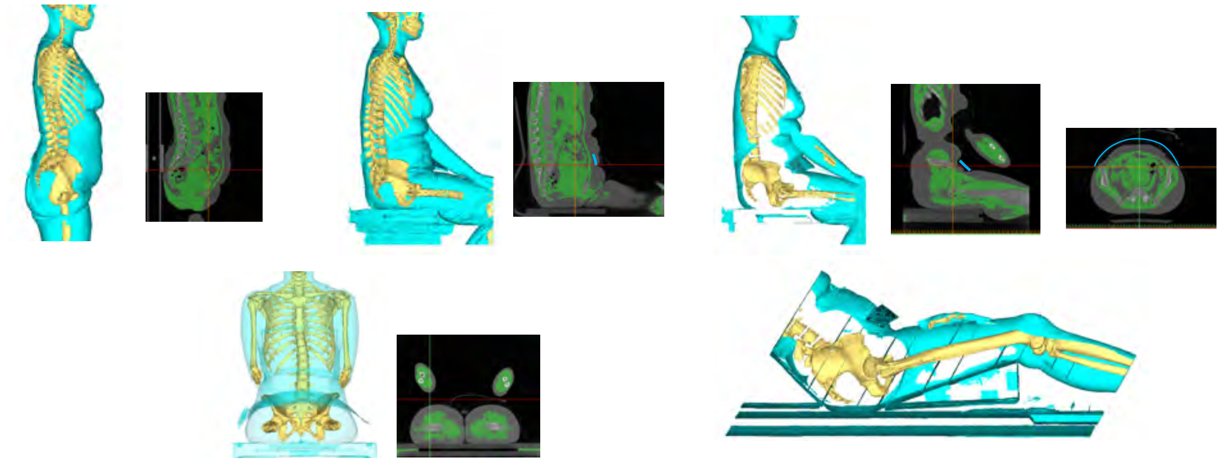

Fig. A16 Female 06 (BMI 21.5)

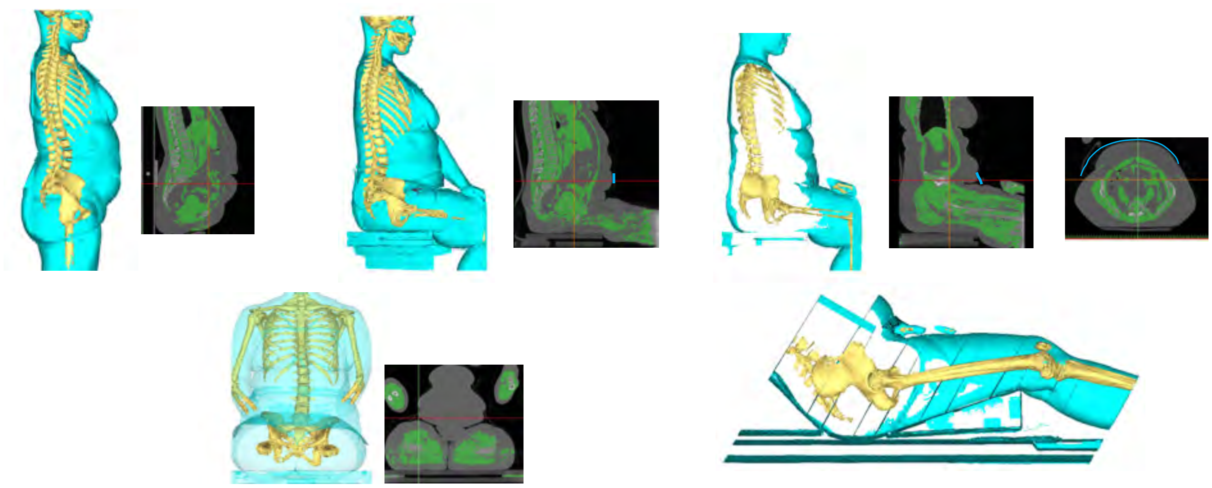

Fig. A17 Female 07 (BMI 31.6)

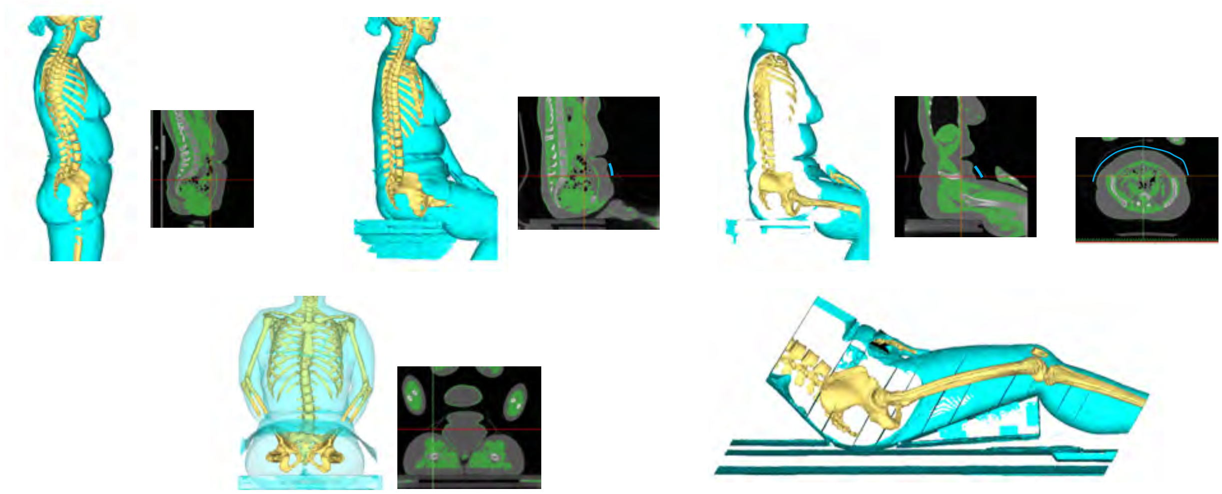

Fig. A18 Female 08 (BMI 26.9)

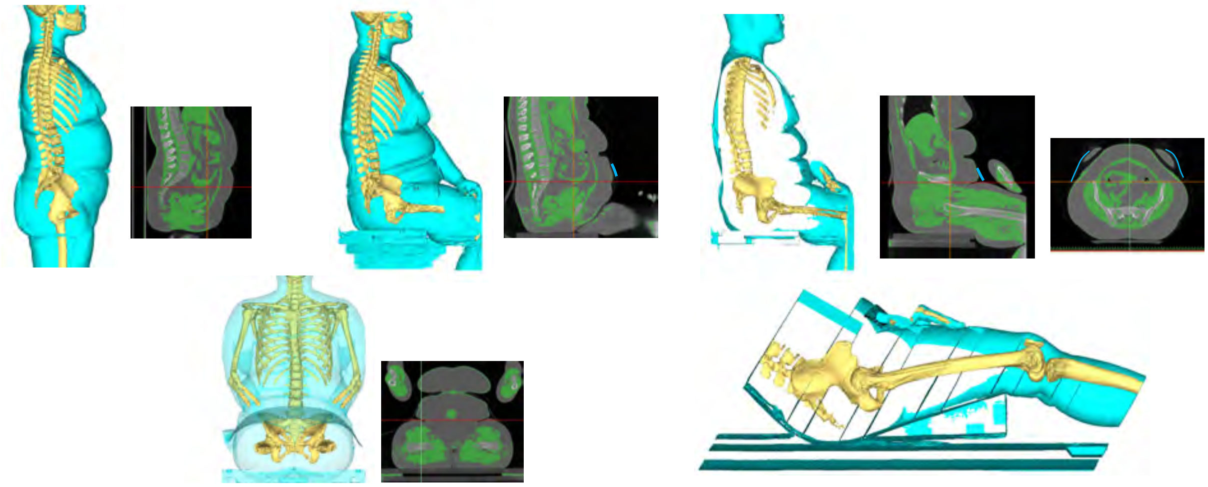

Fig. A19 Female 09 (BMI 31.3)

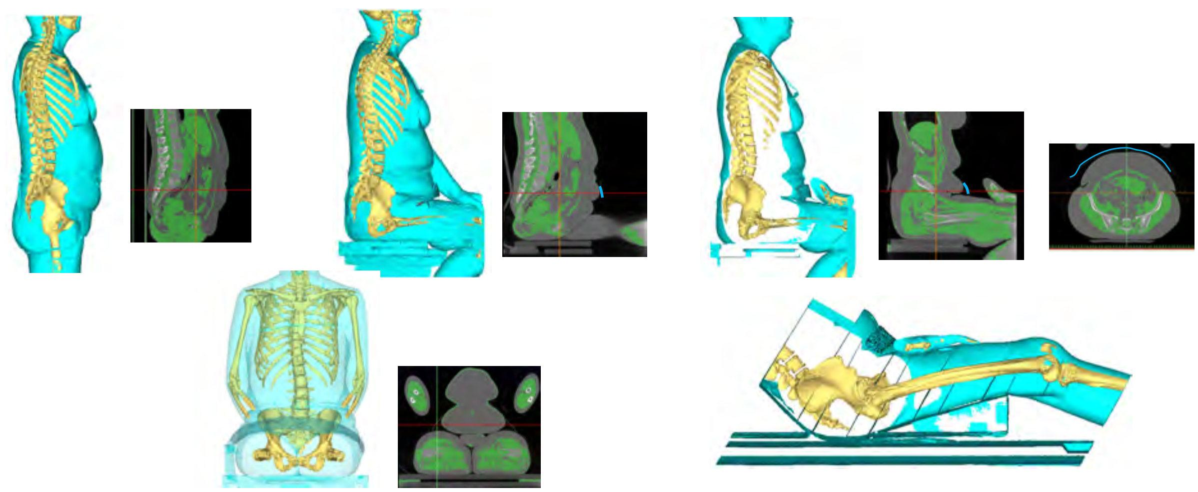

Fig. A20 Female 10 (BMI 26.1)

APPENDIX B ANTHROPOMETRY

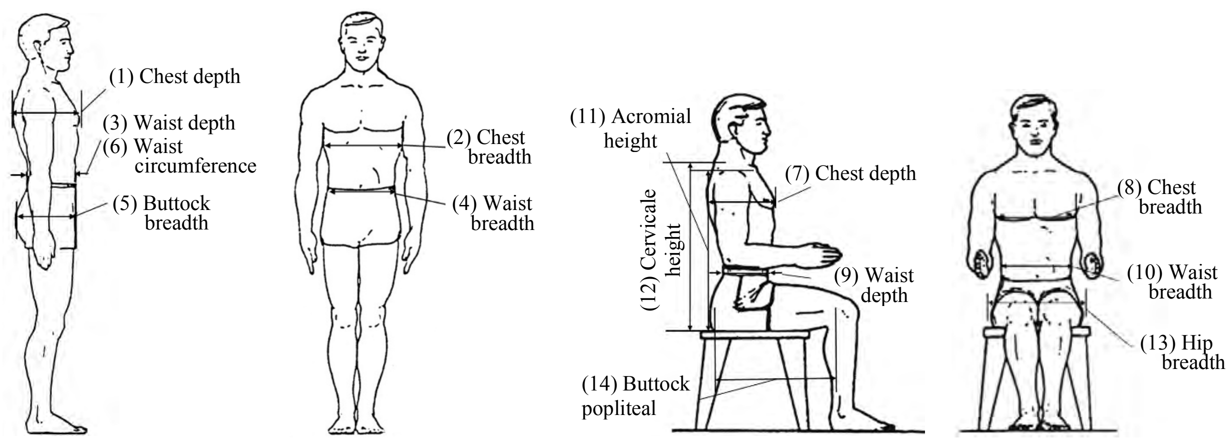

(a) Standing (unit: mm)

Subject (male)	M01	M02	M03	M04	M05	M06	M07	M08	M09	M10
(1) Chest depth	229.1	280.9	189.0	295.1	229.0	291.9	220.9	284.2	239.3	229.1
(2) Chest breadth	312.5	391.9	273.9	390.1	334.5	307.3	339.9	372.1	339.4	327.9
(3) Waist depth	217.0	327.4	178.2	283.9	200.7	308.4	227.1	318.5	233.7	198.5
(4) Waist breadth	282.4	344.9	238.2	331.5	287.4	273.8	288.9	326.5	307.6	266.9
(5) Buttock depth	228.7	307.2	197.7	283.0	238.1	266.6	235.6	275.2	231.0	233.6
(6) Waist circumference at the umbilicus	792.4	1114.7	700.8	1066.1	815.5	892.9	896.5	1070.1	914.4	800.7

Subject (female)	F01	F02	F03	F04	F05	F06	F07	F08	F09	F10
(1) Chest depth	234.9	251.3	197.1	221.0	216.9	234.5	294.5	277.0	294.4	291.6
(2) Chest breadth	304.7	301.5	280.1	273.6	292.0	294.3	365.5	327.8	375.7	350.6
(3) Waist depth	211.8	207.4	205.0	185.3	204.2	214.7	277.8	227.0	295.6	275.8
(4) Waist breadth	253.0	262.2	229.1	242.7	255.2	257.0	344.1	289.2	345.4	322.9
(5) Buttock depth	234.6	245.8	193.6	216.9	213.1	228.2	285.6	242.5	287.2	259.4
(6) Waist circumference at the umbilicus	769.9	817.2	669.7	783.0	787.4	903.6	1177.5	889.3	1020.3	1022.0

(b) Upright sitting (unit: mm)

Subject (male)	M01	M02	M03	M04	M05	M06	M07	M08	M09	M10
(7) Chest depth	236.3	285.8	196.7	303.1	238.3	279.8	NA	NA	233.5	250.6
(8) Chest breadth	337.5	400.4	293.5	402.1	361.7	370.4	339.4	365.4	334.7	341.9
(9) Waist depth	216.3	357.7	188.6	291.0	217.7	289.9	231.6	305.5	216.5	249.8
(10) Waist breadth	283.5	361.9	251.5	336.8	299.9	318.0	305.1	325.0	266.3	315.1
(11) Acromial height	636.5	647.8	605.4	640.9	673.6	646.6	601.8	654.9	606.2	618.6
(12) Cervicale height	662.7	666.5	665.0	660.5	687.0	640.1	638.0	661.5	652.5	652.3
(13) Hip breadth	369.8	427.1	332.6	460.7	394.2	430.9	396.0	401.4	384.1	413.5
(14) Buttock-popliteal	436.4	372.2	389.8	415.0	445.2	416.5	416.1	418.5	433.5	408.6

Subject (female)	F01	F02	F03	F04	F05	F06	F07	F08	F09	F10
(7) Chest depth	237.9	258.2	206.7	237.0	218.1	248.6	309.9	275.9	301.3	290.5
(8) Chest breadth	306.7	319.8	285.9	295.8	299.0	298.7	382.1	345.9	404.8	353.3
(9) Waist depth	222.8	234.3	181.3	203.6	213.4	237.0	293.2	249.2	312.9	280.2
(10) Waist breadth	276.2	277.8	233.7	261.5	264.6	261.6	349.2	291.6	392.1	330.8
(11) Acromial height	556.4	629.4	578.8	591.0	298.2	536.5	601.2	572.6	604.4	662.5
(12) Cervicale height	586.5	655.1	596.2	601.0	627.2	563.9	624.5	583.8	606.0	675.2
(13) Hip breadth	387.4	411.9	320.5	395.0	368.4	385.1	475.5	411.2	416.6	425.0
(14) Buttock-popliteal	439.0	431.5	426.5	428.0	440.7	410.4	426.7	380.6	413.9	429.5

APPENDIX C DATA USED IN FIGURES

	Subject (male)	M01	M02	M03	M04	M05	M06	M07	M08	M09	M10
Table 1	Age	48	21	27	33	30	41	43	36	47	22
Table 1	Standing height (cm)	174.0	171.5	169.2	165.0	179.0	168.0	168.8	171.0	168.0	168.3
Table 1	Weight (kg)	57	98.5	50.5	93	75	78	63	85	70	63.1
Table 1	BMI (kg/cm^2)	18.8	33.5	17.6	34.2	23.4	27.6	22.1	29.1	24.8	22.3
Fig. 10	ASIS width (mm)	248.7	228.3	218.5	235.3	234.5	239.0	228.6	245.2	224.9	239.2
Fig. 10	Pelvis height (mm)	210.5	211.6	204.2	207.6	222.0	214.2	205.6	209.9	213.6	204.5
Fig. 11	Thigh A-P diameter standing (mm)	158.7	228.9	154.2	213.7	198.0	190.6	178.4	190.8	196.1	177.6
Fig. 12(a)	Thigh height (mm)	130.0	181.0	147.2	187.5	170.8	169.8	147.3	181.5	161.6	155.2
Fig. 12(b)	Flesh margin of ischium (mm)	8.4	21.6	14.9	25.0	17.6	18.0	7.2	11.0	11.0	10.5
Fig. 12(c)	ASIS height (mm)	136.6	180.0	158.2	159.4	187.7	168.8	151.7	170.4	157.9	149.8
Fig. 12(d)	ASIS-thigh height (mm)	6.6	-1.0	11.0	-28.1	16.9	-1.0	4.5	-11.1	-3.7	-5.4
Fig. 13	Z-coordinate upright sitting (mm)	79.1	102.2	84.0	93.0	98.5	92.7	78.0	85.5	88.0	83.2
Fig. 13	Z-coordinate reclined (mm)	93.5	107.6	89.9	109.1	106.4	101.8	84.5	104.0	96.5	91.8
Fig. 14	Pelvis angle standing (degree)	-1.6	0.5	-4.0	-1.8	2.6	-6.9	-0.5	-9.3	0.4	-3.8
Fig. 14	Pelvis angle upright (degree)	1.9	-18.5	-18.0	-9.5	-12.5	-15.0	-15.6	-16.2	-16.6	-17.4
Fig. 14	Pelvis angle reclined (degree)	-68.3	-58.3	-70.1	-59.3	-74.9	-68.0	-68.0	-63.9	-72.6	-55.4
Fig. 15	Hip point X-coordinate upright sitting (mm)	108.3	116.5	133.4	127.0	104.6	110.4	121.2	134.4	127.6	127.0
Fig. 15	Hip point Z-coordinate upright sitting (mm)	79.1	102.2	84.0	93.0	98.5	92.7	78.0	85.5	88.0	83.2
Fig. 15	Hip point X-coordinate reclined (mm)	132.9	111.6	108.6	113.2	125.0	112.5	127.4	116.7	139.4	98.1
Fig. 15	Hip point Z-coordinate reclined (mm)	93.5	107.6	89.9	109.1	106.4	101.8	84.5	104.0	96.5	91.8
Fig. 17	Pelvis angle standing (mm)	-1.6	0.5	-4.0	-1.8	2.6	-6.9	-0.5	-9.3	0.4	-3.8
Fig. 17	L3-L5 angle standing (degree)	13.6	26.6	23.4	22.6	23.8	22.2	26.4	27.7	15.6	4.5
Fig. 17	Pelvis angle upright (degree)	1.9	-18.5	-18.0	-9.5	-12.5	-15.0	-15.6	-16.2	-16.6	-17.4
Fig. 17	L3-L5 angle upright (degree)	17.0	13.9	21.3	19.1	22.7	27.2	27.4	12.7	9.2	5.8
Fig. 17	Pelvis angle reclined (degree)	-68.3	-58.3	-70.1	-59.3	-74.9	-68.0	-68.0	-63.9	-72.6	-55.4
Fig. 17	L3-L5 angle reclined (degree)	5.5	14.2	14.0	18.8	-3.7	3.1	16.0	7.0	-0.9	6.4
Fig. 18	ASIS flesh margin standing (mm)	6.8	79.4	7.1	31.5	8.2	30.8	12.4	35.9	14.3	6.7
Fig. 18	ASIS flesh margin upright (mm)	14.1	133.6	11.4	22.6	16.5	57.5	30.7	10.6	32.5	13.3
Fig. 18	ASIS flesh margin reclined (mm)	8.8	107.4	8.9	49.6	12.1	43.5	22.9	19.5	18.3	8.9
Fig. 19	Abdominal depth (mm)	2.5	27.0	0.0	29.5	0.0	4.7	0.0	41.8	0.0	0.0
Fig. 20	Flesh margin of great trochanter standing (mm)	12.1	33.1	10.0	31.5	30.1	28.3	26.3	28.5	23.3	24.2
Fig. 20	Flesh margin of great trochanter upright (mm)	26.8	57.8	21.7	51.2	29.7	42.9	43.9	34.7	36.9	33.1

	Subject (male)	M01	M02	M03	M04	M05	M06	M07	M08	M09	M10
Fig. 20	Flesh margin of great trochanter reclined (mm)	23.5	52.8	23.8	52.3	23.4	46.8	39.0	35.9	38.1	38.4
Fig. 21(a)	ASIS-thigh height upright (mm)	136.6	180.0	158.2	159.4	187.7	168.8	151.7	170.4	157.9	149.8
Fig. 21(a)	Lap belt/ASIS overlap upright (mm)	3.8	9.9	13.7	-20.9	13.7	-10.4	8.7	6.9	-9.3	-15.0
Fig. 21(b)	ASIS-thigh height reclined (mm)	11.4	-32.9	-0.5	-27.1	-3.5	-8.6	-8.5	-14.5	-11.1	-2.4
Fig. 21(b)	Lap belt/ASIS overlap reclined (mm)	-6.9	-58.0	-13.0	-51.3	-11.4	-37.6	-26.4	-26.4	-30.9	-23.3

	Subject (female)	F01	F02	F03	F04	F05	F06	F07	F08	F09	F10
Table 1	Age	33	37	27	25	46	37	48	30	33	46
Table 1	Standing height (cm)	155.0	167.0	160.0	160.0	166.0	157.0	161.0	148.0	160.0	175.0
Table 1	Weight (kg)	55	63	45	54	52	53	82	59	80	80
Table 1	BMI (kg/cm^2)	22.9	22.6	17.6	21.1	18.9	21.5	31.6	26.9	31.3	26.1
Fig. 10	ASIS width (mm)	210.2	241.1	222.7	242.6	257.9	234.2	227.6	221.8	229.4	251.8
Fig. 10	Pelvis height (mm)	188.9	209.3	202.0	191.1	200.9	194.0	198.2	184.0	197.8	213.0
Fig. 11	Thigh A-P diameter standing (mm)	180.7	194.4	144.4	182.8	164.8	184.3	224.3	202.5	223.6	186.1
Fig. 12(a)	Thigh height (mm)	144.0	153.3	122.1	133.5	139.6	131.0	137.3	137.3	163.5	150.1
Fig. 12(b)	Flesh margin of ischium (mm)	11.7	16.3	7.4	12.5	15.3	9.0	22.9	12.6	24.0	13.6
Fig. 12(c)	ASIS height (mm)	149.3	162.0	142.3	152.0	163.7	150.1	153.3	153.3	164.4	167.0
Fig. 12(d)	ASIS-thigh height (mm)	5.8	8.6	20.1	18.5	24.1	19.1	11.0	15.9	0.9	16.9
Fig. 13	Z-coordinate upright sitting (mm)	73.0	83.5	74.1	78.0	88.5	76.0	99.5	84.0	94.2	84.0
Fig. 13	Z-coordinate reclined (mm)	91.7	100.5	74.4	96.7	97.7	86.7	115.7	92.4	104.6	87.6
Fig. 14	Pelvis angle standing (degree)	-3.7	-0.4	-1.8	-6.9	-7.5	3.4	-9.2	-1.7	2.6	-9.9
Fig. 14	Pelvis angle upright (degree)	-26.3	-13.2	-22.4	-27.6	-27.2	-34.2	-27.0	-33.9	-24.4	-6.8
Fig. 14	Pelvis angle reclined (degree)	-66.4	-72.4	-56.7	-65.7	-74.2	-58.9	-61.6	-58.2	-62.8	-72.8
Fig. 15	Hip point X-coordinate upright sitting (mm)	132.5	127.6	137.3	152.0	129.2	152.5	147.1	194.9	156.9	110.1
Fig. 15	Hip point Z-coordinate upright sitting (mm)	73.0	83.5	74.1	78.0	88.5	76.0	99.5	84.0	94.2	84.0
Fig. 15	Hip point X-coordinate reclined (mm)	137.0	127.8	114.8	124.6	117.7	111.9	120.0	110.6	127.2	114.8
Fig. 15	Hip point Z-coordinate reclined (mm)	91.7	100.5	74.4	96.7	97.7	86.7	115.7	92.4	104.6	87.6
Fig. 17	Pelvis angle standing (mm)	-3.7	-0.4	-1.8	-6.9	-7.5	3.4	-9.2	-1.7	2.6	-9.9
Fig. 17	L3-L5 angle standing (degree)	25.0	31.3	9.7	16.4	22.5	33.8	30.1	36.3	10.2	20.5
Fig. 17	Pelvis angle upright (degree)	-26.3	-13.2	-22.4	-27.6	-27.2	-34.2	-27.0	-33.9	-24.4	-6.8
Fig. 17	L3-L5 angle upright (degree)	6.4	31.9	-3.6	2.1	-0.1	1.2	19.8	5.7	3.1	16.4
Fig. 17	Pelvis angle reclined (degree)	-66.4	-72.4	-56.7	-65.7	-74.2	-58.9	-61.6	-58.2	-62.8	-72.8
Fig. 17	L3-L5 angle reclined (degree)	6.7	9.9	3.3	6.3	1.3	19.6	6.8	13.0	4.9	-1.1
Fig. 18	ASIS flesh margin standing (mm)	21.9	10.3	6.9	11.4	4.8	13.8	61.7	28.7	56.3	57.3
Fig. 18	ASIS flesh margin upright (mm)	34.2	19.9	11.2	16.2	6.2	17.4	97.5	39.4	90.9	84.3
Fig. 18	ASIS flesh margin reclined (mm)	24.4	15.2	8.4	9.9	8.4	11.1	70.7	26.3	67.8	77.1
Fig. 19	Abdominal depth (mm)	7.2	3.7	0.0	1.6	0.0	10.5	30.3	0.0	7.4	31.3
Fig. 20	Flesh margin of great trochanter standing (mm)	32.3	44.2	17.3	30.8	28.1	37.0	68.2	44.5	48.5	30.4
Fig. 20	Flesh margin of great trochanter upright (mm)	53.9	61.7	21.8	42.5	40.9	55.3	86.1	68.5	73.6	60.6
Fig. 20	Flesh margin of great trochanter reclined (mm)	51.8	62.1	19.7	48.7	42.9	53.7	88.8	69.6	67.9	57.6
Fig. 21(a)	ASIS-thigh height upright (mm)	149.3	162.0	142.3	152.0	163.7	150.1	153.3	153.3	164.4	167.0
Fig. 21(a)	Lap belt/ASIS overlap upright (mm)	3.6	7.0	13.3	14.7	29.1	21.1	11.8	7.2	-4.6	17.6
Fig. 21(b)	ASIS-thigh height reclined (mm)	-9.6	-6.0	4.3	7.2	1.3	2.1	-13.3	-12.2	-30.8	-2.6
Fig. 21(b)	Lap belt/ASIS overlap reclined (mm)	-17.0	-5.9	-4.8	-0.5	1.2	-15.4	-18.5	-25.8	-38.7	-13.0

APPENDIX D ASIS FLESH MARGIN

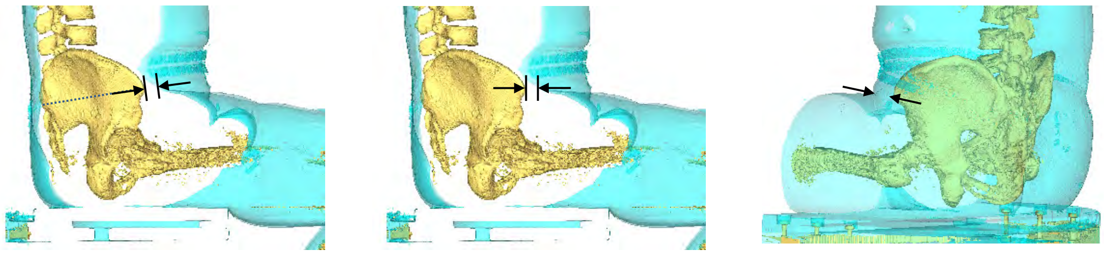

(a) (b) (c)

(a) ASIS-PSIS direction projected on to the sagittal plane across the ASIS

Subject (male)	M01	M02	M03	M04	M05	M06	M07	M08	M09	M10
Standing (mm)	6.8	79.4	7.1	31.5	8.2	30.8	12.4	35.9	14.3	6.7
Upright sitting (mm)	14.1	133.6	11.4	22.6	16.5	57.5	30.7	10.6	32.5	13.3
Reclined (mm)	8.8	107.4	8.9	49.6	12.1	43.5	22.9	19.5	18.3	8.9

Subject (female)	F01	F02	F03	F04	F05	F06	F07	F08	F09	F10
Standing (mm)	21.9	10.3	6.9	11.4	4.8	13.8	61.7	28.7	56.3	57.3
Upright sitting (mm)	34.2	19.9	11.2	16.2	6.2	17.4	97.5	39.4	90.9	84.3
Reclined (mm)	24.4	15.2	8.4	9.9	8.4	11.1	70.7	26.3	67.8	77.1

(b) *x*-direction on the sagittal plane across the ASIS

Subject (male)	M01	M02	M03	M04	M05	M06	M07	M08	M09	M10
Standing (mm)	4.9	79.7	6.2	28.5	7.0	30.6	11.2	32.8	10.9	7.6
Upright sitting (mm)	17.2	95.8	11.8	35.1	14.2	60.9	29.2	9.8	31.0	23.4

Subject (female)	F01	F02	F03	F04	F05	F06	F07	F08	F09	F10
Standing (mm)	21.5	10.1	6.5	11.5	6.9	12.5	62.1	28.3	58.0	48.2
Upright sitting (mm)	27.3	18.4	11.3	17.8	10.0	17.4	95.3	51.1	59.8	90.0

(c) Minimum distance in three dimensions

Subject (male)	M01	M02	M03	M04	M05	M06	M07	M08	M09	M10
Standing (mm)	4.3	45.9	5.5	21.6	6.1	20.6	9.2	20.9	9.1	6.4
Upright sitting (mm)	10.5	71.4	7.1	29.0	11.1	39.4	20.0	15.2	22.0	10.9
Reclined (mm)	5.8	59.0	5.7	31.0	6.7	21.5	14.9	12.2	10.9	7.7

Subject (female)	F01	F02	F03	F04	F05	F06	F07	F08	F09	F10
Standing (mm)	17.5	8.6	6.6	10.2	3.8	9.5	40.7	22.3	43.2	35.2
Upright sitting (mm)	21.0	14.8	7.1	15.5	5.7	13.0	49.4	37.3	53.9	49.2
Reclined (mm)	18.4	11.4	6.5	8.5	5.9	10.7	44.7	21.2	49.9	51.5

APPENDIX E COORDINATES

(a) Standing posture (unit: mm)

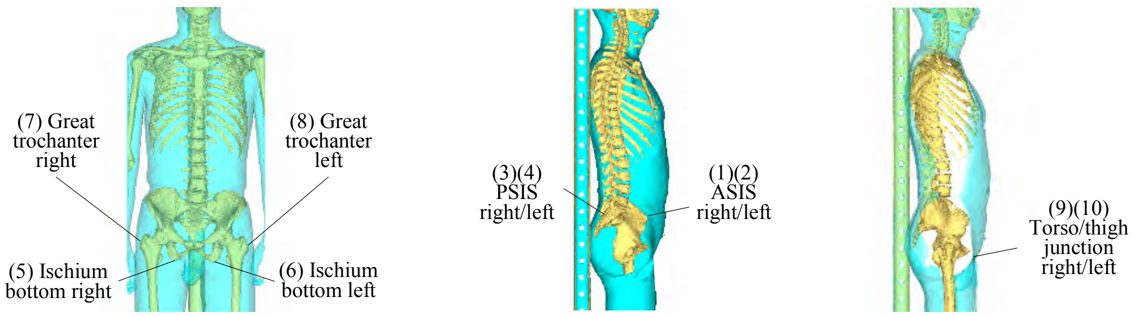

(a) Front view (b) Side view (c) Sagittal plane at the ASIS

Origin: x, y: cylinder center, z: initial measurement position of gantry

Subject (male)		M01	M02	M03	M04	M05	M06	M07	M08	M09	M10
1) ASIS right	X	64.1	9.5	36.4	69.0	73.3	68.5	50.1	126.0	63.5	77.4
	Y	-123.2	-109.0	-113.8	-120.7	-97.3	-127.5	-121.3	-138.2	-123.6	-131.1
	Z	-788.5	-792.8	-840.7	-764.0	-765.5	-713.0	-839.3	-736.9	-733.9	-729.1
2) ASIS left	X	60.0	12.3	56.5	75.2	53.4	69.8	60.3	123.4	60.7	90.9
	Y	120.8	114.6	100.8	111.6	136.0	110.6	104.8	104.0	105.7	104.8
	Z	-795.8	-795.5	-831.1	-765.5	-749.2	-719.5	-843.9	-724.4	-739.5	-736.4
3) PSIS right	X	63.1	10.5	45.6	73.3	61.3	74.5	51.1	138.0	59.2	86.0
	Y	-30.9	-22.1	-29.0	-32.8	-6.5	-40.3	-36.5	-36.9	-38.7	-43.6
	Z	-881.0	-884.0	-922.0	-836.5	-856.5	-799.3	-931.4	-812.0	-818.5	-805.0
4) PSIS left	X	63.5	8.3	50.8	74.9	57.0	81.0	55.1	135.7	59.8	89.4
	Y	20.7	28.7	21.8	18.9	52.1	14.0	16.9	19.9	16.9	15.2
	Z	-878.5	-884.0	-918.1	-833.4	-854.0	-797.0	-929.0	-811.0	-823.5	-803.3
5) Ischium bottom right	X	-23.3	-67.2	-42.2	-12.9	-29.2	-17.9	-30.0	59.5	-27.0	-12.9
	Y	-63.7	-46.6	-45.9	-43.4	-40.7	-52.0	-46.5	-52.1	-55.5	35.4
	Z	-924.5	-940.0	-964.3	-887.0	-899.0	-848.7	-969.5	-879.5	-863.3	-862.3
6) Ischium bottom left	X	-24.3	-69.7	-32.3	-15.3	-30.8	-10.6	-27.0	65.3	-30.4	3.3
	Y	52.0	51.1	45.1	39.3	70.2	35.4	32.6	43.5	33.6	-53.5
	Z	-929.5	-939.5	-963.5	-885.0	-896.0	-855.5	-971.0	-874.5	-864.5	-857.0
7) Great trochanter right	X	-13.8	-50.4	-26.0	6.2	-2.5	0.6	-1.6	79.5	-4.5	14.0
	Y	-159.7	-146.5	-142.5	-155.4	-138.6	-156.6	-150.1	-163.4	-159.3	-162.3
	Z	-872.6	-897.0	-909.1	-837.1	-839.6	-793.0	-920.5	-820.1	-800.9	-804.3
8) Great trochanter left	X	-7.4	-57.4	-19.1	11.0	-17.3	4.2	-5.4	63.9	-5.6	20.8
	Y	149.4	150.8	138.3	141.8	168.1	133.3	135.4	145.4	136.0	134.4
	Z	-881.3	-898.1	-916.4	-828.0	-842.0	133.3	-925.1	-808.1	-807.1	-807.6
9) Torso/thigh junction right in the sagittal plane at the ASIS	X	74.0	65.1	47.7	108.7	84.0	100.7	68.7	157.0	75.3	77.6
	Y	119.3	-108.6	-112.2	-119.7	-96.3	-124.6	-120.8	-136.4	108.6	-131.7
	Z	-878.5	-898.8	-899.6	-847.0	-853.1	-792.5	-881.4	-818.9	-785.1	-705.1
10) Torso/thigh junction left in the sagittal plane at the ASIS	X	75.6	58.8	60.3	119.6	68.3	94.0	72.5	159.3	78.1	93.0
	Y	120.7	119.1	100.9	114.2	139.2	113.6	106.0	104.7	-123.1	104.8
	Z	-890.5	-897.1	-903.6	-868.1	-858.2	-792.1	-908.1	-820.2	-781.1	-715.8

Subject (female)		F01	F02	F03	F04	F05	F06	F07	F08	F09	F10
1) ASIS right	X	61.0	77.5	49.7	48.6	61.2	54.6	81.4	77.0	94.3	58.2
	Y	-114.8	-119.7	-117.8	-122.7	-111.9	-131.3	-120.1	-93.6	-116.7	-120.0
	Z	-757.6	-740.9	-726.6	-738.9	-688.5	-717.0	-708.0	-791.7	-759.5	-656.7
2) ASIS left	X	86.8	89.4	60.1	61.8	51.9	67.2	68.7	66.2	84.4	55.2
	Y	96.0	121.4	106.1	117.6	138.0	104.8	109.3	125.3	109.6	131.2
	Z	-762.3	-744.5	-718.5	-738.2	-687.5	-708.0	-704.0	-783.6	-752.4	-657.0
3) PSIS right	X	72.5	84.0	50.8	63.4	70.6	53.8	91.2	75.2	85.9	75.6
	Y	-43.5	-24.0	-24.1	-34.8	-17.3	-36.6	-24.1	-9.4	-34.7	-8.3
	Z	-846.5	-830.1	-799.5	-823.0	-781.2	-789.9	-795.5	-875.0	-838.3	-767.4
4) PSIS left	X	82.6	85.0	55.8	65.5	66.6	57.2	85.1	73.2	85.5	75.1
	Y	12.1	35.5	6.2	33.5	41.3	24.8	26.7	35.4	24.8	-5.5
	Z	-852.3	-828.6	-793.3	-821.5	-779.5	-790.0	-804.6	-871.8	-837.4	-766.5
5) Ischium bottom right	X	-9.6	-3.6	-22.1	-13.3	-12.3	-31.1	10.0	6.6	9.3	-2.6
	Y	-62.2	63.8	-61.4	-49.4	-48.0	-60.4	-73.8	-50.5	-63.6	-51.4
	Z	-882.5	-873.5	-838.5	-865.0	-829.5	-823.5	-847.0	-916.5	-875.0	-813.3
6) Ischium bottom left	X	6.2	-4.6	-16.2	-15.8	-20.2	-24.1	12.3	3.2	7.2	-9.8
	Y	48.2	-55.3	56.5	60.7	70.6	56.1	55.4	77.4	52.2	60.7
	Z	-884.5	-871.5	-838.5	-864.5	-827.0	-821.7	-850.0	-916.5	-876.0	-812.5
7) Great trochanter right	X	9.1	17.9	1.2	13.0	4.3	-5.6	30.7	31.7	24.6	8.0
	Y	-142.8	-134.8	-145.8	-141.5	-134.9	-143.5	-149.5	-122.4	-142.1	-152.6
	Z	-838.3	-821.2	-797.5	-826.0	-778.3	-776.1	-795.1	-871.4	-829.0	-753.9
8) Great trochanter left	X	38.5	23.8	14.1	32.6	-1.4	12.1	20.1	31.6	22.8	8.1
	Y	129.8	145.1	137.3	143.8	149.9	130.0	140.9	147.0	131.9	158.9
	Z	-847.1	-829.0	-793.4	-824.1	-778.6	-777.5	-799.9	-871.2	-833.5	-761.4
9) Torso/thigh junction right in the sagittal plane at the ASIS	X	78.0	100.9	58.3	66.7	66.5	113.6	114.6	96.4	121.4	89.8
	Y	-116.7	119.2	-118.7	-120.7	-113.8	-128.5	-120.0	-92.5	-116.9	-119.7
	Z	-830.0	-780.7	-747.2	-797.9	-761.6	-779.0	-770.9	-857.2	-823.6	-748.0
10) Torso/thigh junction left in the sagittal plane at the ASIS	X	98.0	91.1	67.0	77.4	55.2	72.9	108.2	85.9	116.5	87.0
	Y	96.2	-116.8	104.8	118.4	139.9	103.9	113.6	129.4	108.7	131.1
	Z	-830.9	-773.0	-751.5	-790.5	-756.0	-770.8	-771.5	-853.4	-821.0	-735.9

(b) Upright sitting posture (unit: mm)

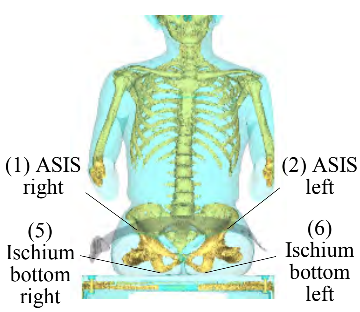

(a) Front view

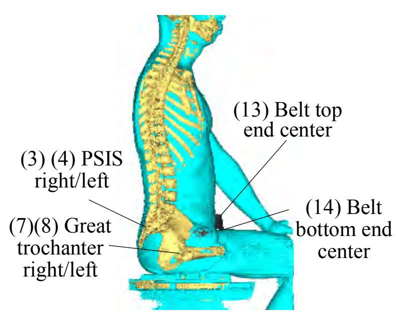

(b) Side view

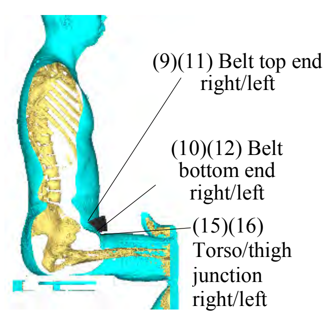

(c) Sagittal plane at the ASIS

Origin: Seat cross line (center); Buckle anchor x=-30.0, y=-244.8, z=-93.8; Lap outer anchor x=42.1, y=253.3, z=23.6;
Lap belt start point (right) x=22.2, y=-250, z=28.0; (left) x=42.1, y=250, z=23.6

Subject (male)		M01	M02	M03	M04	M05	M06	M07	M08	M09	M10
1) ASIS right	X	164.9	148.4	164.5	175.2	147.8	157.9	150.5	165.4	152.3	166.3
	Y	-112.5	-111.5	-89.9	-102.7	-130.1	-130.1	-131.0	-100.9	-120.4	-119.2
	Z	142.5	187.5	152.0	160.0	177.1	174.6	156.8	163.7	162.0	152.9
2) ASIS left	X	153.5	140.5	162.9	159.1	137.9	153.5	145.0	158.8	152.6	151.8
	Y	137.5	112.8	129.6	131.5	105.2	106.1	99.3	143.3	109.1	118.8
	Z	145.0	185.0	155.3	168.0	183.8	160.9	157.2	179.4	160.5	158.9
3) PSIS right	X	19.2	10.8	30.5	26.9	6.7	16.5	15.7	17.0	11.3	18.6
	Y	-32.4	-42.2	-29.3	-33.4	-55.9	-59.8	-59.4	-15.8	-42.2	-48.2
	Z	157.0	150.4	153.0	171.7	163.9	171.6	139.7	154.7	151.0	133.9
4) PSIS left	X	19.6	5.9	31.7	404.8	0.5	21.2	12.7	17.0	10.0	13.7
	Y	58.3	38.4	63.3	52.5	27.1	22.0	19.8	59.4	34.0	32.9
	Z	137.0	152.8	151.0	180.2	165.5	158.9	144.7	159.5	152.0	131.4
5) Ischium bottom right	X	68.0	121.1	105.5	99.9	83.9	84.5	101.5	117.3	104.4	108.2
	Y	-49.9	-55.1	-34.3	-33.3	-76.4	-62.8	-60.7	-16.7	-53.1	-50.2
	Z	14.9	25.0	12.0	27.4	20.5	28.8	11.0	14.5	13.5	14.5
6) Ischium bottom left	X	71.9	107.4	115.6	94.6	78.2	93.1	95.5	119.6	100.9	108.6
	Y	66.1	52.4	70.3	58.3	45.6	26.1	23.2	79.7	40.7	51.4
	Z	11.5	25.4	12.4	33.4	21.0	21.0	9.5	19.0	13.5	15.5
7) Great trochanter right	X	133.7	145.5	150.6	151.3	128.2	115.2	133.5	144.4	134.7	149.3
	Y	-139.2	-146.7	-121.2	-147.3	-159.8	-160.3	-166.2	-127.5	-156.4	-157.7
	Z	41.0	82.0	43.0	73.0	54.4	71.0	52.5	68.1	53.0	58.0
8) Great trochanter left	X	127.1	113.5	154.5	129.8	118.1	115.2	129.8	143.5	125.0	145.5
	Y	170.6	139.2	153.2	170.1	138.4	127.8	132.8	178.8	137.4	151.3
	Z	43.5	84.0	39.5	78.7	61.5	65.8	56.5	74.0	54.5	56.9
9) Belt top end right	X	189.4	279.3	195.4	237.0	171.8	228.5	175.9	234.3	196.2	162.9
	Y	-111.5	-112.1	-89.5	-102.8	-131.0	-129.2	-131.0	-98.9	-120.2	-119.2
	Z	163.1	210.8	170.0	217.5	210.5	215.6	175.9	200.0	194.3	197.0
10) Belt bottom end right in the sagittal plane at the ASIS	X	226.0	306.9	228.7	266.5	204.0	255.2	213.7	265.1	233.1	196.3
	Y	-111.5	-112.4	-88.0	-103.2	-130.7	-130.0	-131.0	-99.8	-120.2	-119.2
	Z	132.4	174.0	138.5	182.0	177.4	178.9	145.7	160.9	166.6	164.4
11) Belt top end left in the sagittal plane at the ASIS	X	178.9	276.4	198.4	226.5	177.6	222.4	175.5	227.4	197.9	157.1
	Y	140.2	113.9	130.6	131.6	105.4	106.2	99.3	143.8	107.8	118.8
	Z	163.5	209.5	176.0	218.4	208.5	215.0	173.5	200.0	198.9	196.0
12) Belt bottom end left in the sagittal plane at the ASIS	X	221.2	306.6	224.7	255.8	208.8	254.7	212.8	267.4	237.6	197.0
	Y	139.3	113.0	129.4	131.6	106.2	107.1	98.4	143.2	109.6	118.8
	Z	136.0	173.3	138.5	181.5	176.1	181.3	142.9	170.3	173.4	169.9
13) Belt top end center in the midsagittal plane	X	238.5	328.8	230.1	277.5	201.2	270.4	227.4	284.3	246.2	201.8
	Y	12.3	9.5	13.2	7.1	-3.6	-5.1	-8.0	10.0	-5.1	8.6
	Z	182.1	216.0	188.5	230.9	221.9	239.4	193.0	213.5	218.0	221.4
14) Belt bottom end center in the midsagittal plane	X	244.8	323.6	241.9	284.9	215.9	290.9	236.6	288.7	258.9	221.9
	Y	14.5	9.5	13.5	6.8	-3.1	-5.5	-10.0	12.4	-6.0	8.5
	Z	136.5	171.2	144.0	185.5	179.5	198.4	148.5	167.8	174.0	180.4
15) Torso/thigh junction right in the sagittal plane at the ASIS	X	197.6	246.9	205.2	194.2	165.0	213.8	177.7	227.0	185.5	190.0
	Y	-111.4	-111.0	-87.9	-103.7	-130.1	-130.3	-131.1	-100.8	-119.3	-117.7
	Z	131.5	187.5	130.5	184.0	176.5	163.5	154.9	165.4	163.0	153.5
16) Torso/thigh junction left in the sagittal plane at the ASIS	X	166.6	236.2	192.8	182.4	160.1	213.3	175.7	218.9	190.6	184.5
	Y	138.3	113.9	131.3	132.5	106.1	106.1	98.4	143.3	108.3	119.1
	Z	151.4	187.4	139.0	191.0	173.1	160.5	147.4	172.9	164.1	156.4

Subject (female)		F01	F02	F03	F04	F05	F06	F07	F08	F09	F10
1) ASIS right	X	149.6	158.1	168.0	162.6	144.7	163.9	165.4	192.9	187.0	151.9
	Y	-112.4	-127.1	-115.2	-108.7	-113.3	-134.9	-125.2	-125.1	-111.5	-113.4
	Z	152.2	163.4	139.4	155.5	171.5	148.9	188.4	156.4	166.4	167.0
2) ASIS left	X	149.8	174.7	159.9	164.7	151.1	166.7	168.7	183.3	181.7	156.6
	Y	102.5	112.0	108.2	129.6	145.1	100.3	98.4	92.5	117.9	136.4
	Z	156.6	162.2	144.0	155.1	167.5	156.7	171.0	154.4	168.5	168.0
3) PSIS right	X	14.6	23.4	18.5	32.1	13.2	40.2	23.5	75.2	36.0	13.9
	Y	-48.9	-42.1	-56.9	-29.9	-35.3	-51.7	-60.7	-66.5	-39.2	-31.4
	Z	136.5	150.5	133.6	127.7	131.4	91.5	148.0	109.0	147.5	174.2
4) PSIS left	X	17.9	25.6	18.9	30.3	14.5	39.4	32.7	80.3	40.2	13.1
	Y	40.4	56.4	40.7	62.3	67.0	32.1	42.8	28.7	36.9	59.3
	Z	138.5	159.2	122.6	123.9	134.6	93.0	124.5	96.5	140.2	178.9
5) Ischium bottom right	X	118.1	108.6	127.0	141.7	115.7	148.8	135.0	192.6	150.6	82.3
	Y	-66.7	-64.5	-67.7	-41.3	-45.0	-77.7	-83.1	-88.0	-58.4	-44.7
	Z	12.0	16.0	9.7	13.3	17.0	10.6	32.2	14.2	28.0	15.6
6) Ischium bottom left	X	114.4	109.5	126.3	142.8	121.3	149.5	143.8	193.7	159.4	84.6
	Y	57.7	58.3	59.7	72.9	77.9	51.3	47.1	47.2	62.3	67.6
	Z	14.0	15.5	9.5	13.5	16.5	12.0	20.3	12.0	25.0	15.5
7) Great trochanter right	X	157.4	147.7	166.2	175.1	149.6	170.0	170.1	216.9	176.9	122.1
	Y	-139.6	-145.1	-141.0	-128.1	-119.3	-146.8	-162.4	-151.5	-134.7	-144.7
	Z	56.9	69.5	61.7	57.5	52.3	51.0	83.6	61.2	72.9	60.5
8) Great trochanter left	X	157.8	161.5	161.3	171.1	151.6	173.0	168.2	206.2	176.8	136.0
	Y	132.0	139.9	135.9	157.3	146.7	121.1	129.7	112.8	140.8	165.9
	Z	56.6	65.7	61.3	65.2	48.7	61.2	72.3	59.5	82.5	60.5
9) Belt top end right	X	186.7	176.1	175.7	192.0	178.9	187.3	259.5	240.1	272.7	252.1
	Y	-110.5	-126.2	-113.4	-107.5	-112.1	-134.6	-124.2	-124.5	-112.6	-112.4
	Z	181.5	186.0	169.0	170.5	168.0	160.7	212.5	186.1	212.5	194.7
10) Belt bottom end right in the sagittal plane at the ASIS	X	220.1	213.1	207.2	224.6	218.9	225.2	277.8	266.7	292.2	272.2
	Y	-110.5	-126.1	-113.0	-107.5	-112.4	-132.8	-124.0	-124.1	-110.5	-112.4
	Z	148.5	155.3	133.4	137.9	141.0	130.0	168.5	149.0	172.0	153.6
11) Belt top end left in the sagittal plane at the ASIS	X	186.7	187.7	179.9	186.7	189.2	187.7	268.7	245.6	267.6	250.4
	Y	102.3	112.6	107.9	131.6	145.2	102.1	100.3	92.6	117.9	136.5
	Z	176.0	188.0	166.0	175.1	169.0	163.0	203.0	184.5	210.0	185.5
12) Belt bottom end left in the sagittal plane at the ASIS	X	222.9	223.1	205.9	220.5	220.1	225.6	287.2	264.2	290.2	279.2
	Y	102.5	113.1	109.2	129.6	145.2	101.7	100.3	92.5	118.3	136.2
	Z	146.6	155.5	127.5	141.0	134.0	134.0	159.5	143.0	168.5	148.5
13) Belt top end center in the midsagittal plane	X	226.3	232.8	204.7	225.4	232.5	244.6	303.4	282.5	312.2	294.7
	Y	-6.0	-2.1	8.0	31.1	19.6	-9.7	-16.3	-18.7	-0.5	2.7
	Z	196.5	202.0	178.5	188.0	191.0	185.0	210.5	197.5	226.0	204.0
14) Belt bottom end center in the midsagittal plane	X	239.4	237.3	220.4	236.7	244.4	256.5	302.2	291.9	324.9	305.8
	Y	-6.3	-2.1	7.9	11.2	21.8	-10.2	-15.8	-16.9	5.5	6.7
	Z	152.9	156.0	135.5	143.8	145.5	141.6	164.5	152.5	181.5	158.5
15) Torso/thigh junction right in the sagittal plane at the ASIS	X	188.1	172.3	181.9	192.6	177.9	204.1	243.0	244.5	247.3	210.5
	Y	-111.2	-126.1	-113.4	-108.5	-111.4	-133.8	-124.1	-124.1	-111.5	-112.4
	Z	141.9	165.0	136.6	140.0	137.0	128.0	176.0	145.5	165.0	151.5
16) Torso/thigh junction left in the sagittal plane at the ASIS	X	193.4	195.4	179.9	199.4	181.7	206.3	224.7	240.4	237.3	209.2
	Y	102.3	113.0	108.4	131.5	145.2	101.2	100.3	92.3	118.9	136.5
	Z	141.0	159.9	135.0	135.5	133.0	130.0	161.5	140.0	165.5	149.5

(c) Reclined sitting posture (unit: mm)

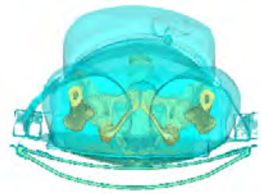

(a) Front view

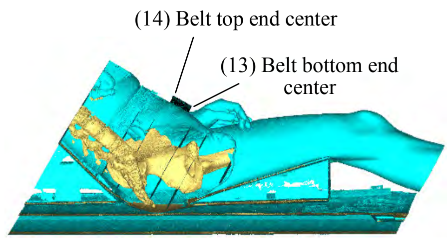

(b) Side view

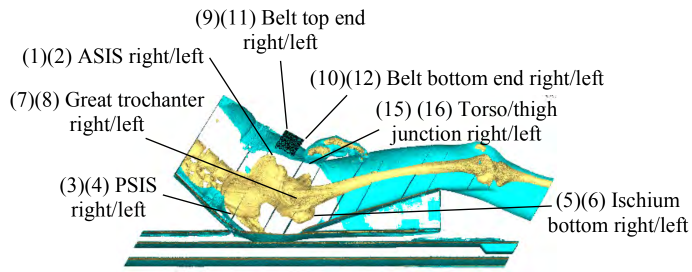

(c) Sagittal plane at the ASIS

Origin: seat cross line (center), Anchor position x=-16.3, y=-244.8, z=-114.9; Lap outer anchor x=55.7, y=253.3, z=2.5;
Lap belt start point (right) x=41.9, y=-225.7, z=9.9; (left) x=56.0, y=253.3, z=9.9

Subject (male)		M01	M02	M03	M04	M05	M06	M07	M08	M09	M10
1) ASIS right	X	82.0	68.2	66.1	81.8	64.1	69.2	83.0	74.7	91.7	81.6
	Y	-92.3	-92.9	-85.3	-97.7	-96.6	-101.6	-108.8	-77.1	-90.7	-102.4
	Z	158.7	188.3	128.5	176.8	178.6	190.1	149.1	167.3	158.6	165.3
2) ASIS left	X	74.2	63.8	41.8	70.4	49.0	67.1	77.1	83.0	82.3	72.4
	Y	152.6	128.7	120.6	131.7	138.6	133.7	123.0	167.9	136.7	130.9
	Z	142.1	180.8	179.0	164.2	170.6	171.3	141.9	161.6	158.4	153.4
3) PSIS right	X	-6.0	-17.4	-21.3	-21.6	-8.5	-21.2	5.8	-13.0	18.1	-24.7
	Y	-20.1	-24.5	-11.4	-28.5	-32.2	-35.8	-40.0	8.8	-13.7	45.0
	Z	32.3	70.2	42.2	69.5	49.8	73.3	35.7	48.6	36.2	52.4
4) PSIS left	X	5.2	-18.2	-29.8	-24.9	-8.1	-22.7	3.5	-6.6	10.8	-27.7
	Y	64.8	53.4	78.5	52.7	61.5	49.7	42.0	87.0	58.6	-39.8
	Z	19.6	66.7	42.6	62.2	42.3	65.0	32.7	47.6	35.2	60.5
5) Ischium bottom right	X	170.7	147.3	138.3	137.9	155.5	130.3	160.0	153.8	181.8	122.3
	Y	-34.9	-47.0	-13.1	-35.9	-47.9	-44.1	-39.9	-12.7	-18.5	-39.0
	Z	23.8	39.6	19.7	36.0	38.5	36.4	17.7	27.0	33.7	19.7
6) Ischium bottom left	X	172.4	144.4	127.8	133.5	150.2	139.6	160.0	163.0	175.4	125.2
	Y	85.6	75.4	95.0	60.2	86.8	59.2	45.9	88.9	74.3	54.9
	Z	19.0	34.7	14.6	32.6	31.5	36.5	13.8	28.0	30.5	18.3
7) Great trochanter right	X	147.8	133.2	126.0	125.5	138.1	115.9	145.2	125.6	139.7	126.3
	Y	-121.7	-131.4	-95.9	-128.7	-124.0	-128.9	-143.2	-105.3	-117.5	-138.2
	Z	43.4	88.5	54.4	67.9	60.8	69.6	73.1	61.0	77.9	62.7
8) Great trochanter left	X	135.4	124.8	112.1	106.2	129.1	105.6	141.7	141.9	138.1	110.8
	Y	170.7	160.8	178.2	152.2	157.1	149.9	148.5	189.1	167.0	155.2
	Z	38.1	76.6	40.6	50.8	49.3	70.8	60.1	54.8	62.0	54.8
9) Belt top end right in the sagittal plane at the ASIS	X	89.5	131.3	71.2	89.3	67.9	96.3	71.7	89.8	71.8	63.4
	Y	-90.9	-92.9	137.4	-98.6	-96.6	-100.6	-110.6	-76.0	-91.7	-99.5
	Z	177.7	268.8	128.5	240.6	203.0	241.8	183.9	203.6	198.8	201.8

Subject (male)		M01	M02	M03	M04	M05	M06	M07	M08	M09	M10
10) Belt bottom end right in the sagittal plane at the ASIS	X	130.5	169.3	112.7	131.4	109.1	134.1	116.6	131.2	113.9	106.1
	Y	-90.2	-93.9	-94.1	-97.6	-95.7	-100.4	-110.2	-75.2	-92.4	-99.5
	Z	158.5	241.8	128.6	222.8	186.5	219.2	175.8	185.0	181.1	184.2
11) Belt top end left in the sagittal plane at the ASIS	X	82.8	134.8	71.3	87.0	57.9	92.3	78.7	99.5	77.5	54.7
	Y	151.5	129.6	135.6	129.8	140.0	135.5	123.3	169.4	136.0	130.8
	Z	158.0	262.9	179.0	238.8	191.9	228.8	175.1	202.1	202.2	182.7
12) Belt bottom end left in the sagittal plane at the ASIS	X	128.2	168.5	115.9	129.7	101.7	136.5	121.2	138.1	122.8	101.5
	Y	152.6	130.3	124.6	129.8	139.5	135.6	123.0	168.9	135.8	130.8
	Z	148.7	228.4	178.2	221.9	179.7	217.9	163.7	181.0	193.6	181.9
13) Belt top end center in the midsagittal plane	X	111.4	NA	89.7	115.2	79.1	121.2	101.9	132.2	99.7	76.1
	Y	32.6	NA	51.1	23.4	18.5	15.8	3.9	34.2	29.3	10.8
	Z	210.5	NA	197.6	276.7	234.5	281.9	230.4	245.8	250.6	225.9
14) Belt bottom end center in the midsagittal plane	X	151.4	NA	127.4	149.2	120.0	159.5	141.7	165.0	139.9	116.7
	Y	32.7	NA	51.6	24.2	19.4	15.6	3.0	34.2	28.4	9.9
	Z	188.8	NA	173.8	247.6	216.2	257.2	206.3	214.6	229.2	205.1
15) Torso/thigh junction right in the sagittal plane at the ASIS	X	123.6	164.9	96.0	131.6	87.0	135.9	121.6	123.6	126.5	114.8
	Y	-91.4	-98.8	-67.1	-97.6	-94.3	-101.5	-105.3	-80.0	-87.9	-104.7
	Z	151.0	219.1	148.5	204.1	185.9	198.4	159.5	178.0	169.7	168.0
16) Torso/thigh junction left in the sagittal plane at the ASIS	X	118.5	145.6	85.9	126.5	102.3	130.1	118.8	152.0	124.9	109.9
	Y	148.8	131.6	152.5	139.6	137.4	136.6	125.0	166.9	137.8	130.9
	Z	139.4	218.4	146.4	190.3	173.1	183.3	148.4	173.2	170.4	158.0

Subject (female)		F01	F02	F03	F04	F05	F06	F07	F08	F09	F10
1) ASIS right	X	98.2	77.8	99.9	87.4	74.1	94.9	85.1	69.9	104.2	49.5
	Y	-97.1	-102.0	-70.5	-86.4	-89.4	-79.4	-122.2	-82.1	-117.3	-98.1
	Z	124.3	162.3	161.5	177.0	166.6	173.5	144.2	152.9	144.4	141.4
2) ASIS left	X	92.6	96.5	88.7	86.4	63.9	82.2	78.1	71.4	84.0	39.4
	Y	125.3	121.0	101.3	116.7	124.1	113.9	145.0	113.1	139.7	134.0
	Z	152.2	173.8	160.1	176.1	199.2	167.3	184.9	179.0	141.1	177.3
3) PSIS right	X	1.1	2.0	-13.1	-1.0	4.1	0.6	-11.5	-6.2	-4.9	-18.3
	Y	-19.1	-32.1	-34.7	-25.4	-13.6	-28.2	-21.4	-18.5	-37.6	-11.2
	Z	46.7	42.7	38.2	57.0	40.2	45.2	77.0	57.8	52.3	24.2
4) PSIS left	X	5.7	23.3	-11.6	-2.6	-2.8	-10.3	-6.2	-2.2	0.1	-28.1
	Y	71.7	71.8	57.2	66.4	79.1	63.7	89.8	91.8	38.6	83.2
	Z	40.2	32.8	34.6	50.3	40.4	41.5	64.7	50.1	41.4	22.4
5) Ischium bottom right	X	169.6	170.8	126.6	147.1	165.9	125.3	156.7	140.8	158.6	155.0
	Y	-35.7	-55.8	-52.2	-41.9	-18.4	-47.9	-32.2	-42.9	-50.3	-13.6
	Z	25.5	36.0	3.0	26.6	38.6	16.4	52.1	25.5	31.6	20.6
6) Ischium bottom left	X	160.0	178.6	134.2	142.1	157.7	117.1	152.9	147.3	154.5	143.1
	Y	86.3	73.7	80.6	81.2	102.5	83.2	99.6	93.8	74.7	104.8
	Z	7.0	24.7	3.2	19.9	33.1	9.6	43.5	21.8	18.4	15.0
7) Great trochanter right	X	151.1	140.9	137.3	137.8	141.6	129.5	137.0	127.8	143.0	116.5
	Y	-108.0	-125.5	-124.0	-125.8	-100.6	-119.8	-109.1	-107.1	-124.7	-114.2
	Z	75.5	90.4	65.2	85.6	82.1	85.2	108.9	84.0	96.3	60.7
8) Great trochanter left	X	156.4	160.6	130.2	136.6	136.3	119.5	139.4	138.6	137.1	110.7
	Y	163.6	158.8	159.7	165.0	176.4	153.1	186.3	161.4	153.0	194.7
	Z	72.4	74.6	67.5	79.5	78.0	75.5	99.2	83.9	79.4	51.1
9) Belt top end right in the sagittal plane at the ASIS	X	98.6	84.8	75.2	87.4	88.7	93.0	133.6	81.0	130.9	102.3
	Y	169.7	153.6	128.5	140.1	139.1	150.8	198.8	169.4	219.7	170.6
	Z	123.9	161.4	159.4	177.3	165.6	174.5	144.2	152.9	142.8	140.5

Subject (female)		F01	F02	F03	F04	F05	F06	F07	F08	F09	F10
10) Belt bottom end right in the sagittal plane at the ASIS	X	138.9	132.4	116.6	130.4	131.8	137.0	170.0	123.7	167.4	140.9
	Y	-110.7	-109.4	-75.5	-84.0	-81.4	-96.3	-136.3	-106.1	-149.4	-104.0
	Z	123.3	160.6	159.4	176.4	164.7	174.4	144.2	152.8	143.4	141.4
11) Belt top end left in the sagittal plane at the ASIS	X	97.5	93.0	78.4	82.8	85.8	108.9	135.2	82.7	131.5	99.4
	Y	159.0	144.8	121.1	133.2	137.1	145.3	192.0	148.5	208.1	170.9
	Z	151.9	175.6	159.3	177.1	200.0	168.7	186.0	180.0	141.1	179.0
12) Belt bottom end left in the sagittal plane at the ASIS	X	141.2	132.4	124.8	127.6	130.6	150.2	168.8	126.6	167.2	141.9
	Y	143.6	121.8	105.5	119.5	125.6	124.6	165.8	133.0	178.5	152.4
	Z	150.9	174.7	159.1	177.4	199.5	167.3	184.5	180.0	142.9	179.2
13) Belt top end center in the midsagittal plane	X	122.7	115.9	93.8	109.9	118.0	132.9	160.8	107.0	155.7	139.9
	Y	27.4	13.2	25.9	24.9	45.4	22.5	38.1	20.6	22.0	46.4
	Z	208.5	220.1	181.3	205.5	219.5	221.2	256.7	223.9	249.6	221.3
14) Belt bottom end center in the midsagittal plane	X	158.6	156.9	133.9	152.0	154.3	168.0	188.0	142.5	190.7	171.1
	Y	28.6	12.3	26.7	23.5	44.8	23.1	38.1	20.5	22.0	45.3
	Z	181.7	192.1	154.5	178.2	192.3	191.9	220.4	194.6	220.2	187.8
15) Torso/thigh junction right in the sagittal plane at the ASIS	X	139.8	101.9	111.8	122.5	124.6	123.7	137.3	114.9	155.8	134.6
	Y	-73.6	-96.1	-96.1	-101.4	-84.0	-103.4	-77.2	-76.1	-93.8	-89.4
	Z	151.2	173.8	139.0	155.5	152.8	147.3	201.6	160.7	191.6	148.8
16) Torso/thigh junction left in the sagittal plane at the ASIS	X	139.1	123.7	105.3	119.0	109.8	122.8	138.2	108.6	142.2	128.0
	Y	143.7	145.0	128.4	141.6	170.9	135.5	152.5	145.5	136.1	167.4
	Z	135.9	152.6	132.3	147.1	145.3	136.9	193.1	150.9	172.1	146.0